研究成果の刊行物・別刷

Neurobiology of Disease

A Seed for Alzheimer Amyloid in the Brain

Hideki Hayashi,[1] Nobuyuki Kimura,[2] Haruyasu Yamaguchi,[3] Kazuhiro Hasegawa,[4] Tatsuki Yokoseki,[5] Masao Shibata,[5] Naoki Yamamoto,[1] Makoto Michikawa,[1] Yasuhiro Yoshikawa,[2] Keiji Terao,[6] Katsumi Matsuzaki,[7] Cynthia A. Lemere,[8] Dennis J. Selkoe,[8] Hironobu Naiki,[4] and Katsuhiko Yanagisawa[1]

[1]Department of Dementia Research, National Institute for Longevity Sciences, Obu 474-8522, Japan, [2]Department of Biomedical Science, Graduate School of Agricultural and Life Sciences, The University of Tokyo, Bunkyo-ku, Tokyo 113-8657, Japan, [3]Gunma University School of Health Sciences, Maebashi 371-8514, Japan, [4]Division of Molecular Pathology, Department of Pathological Sciences, Faculty of Medical Sciences, University of Fukui, Matsuoka 910-1193, Japan, [5]Department of Pharmaceutical Development, Ina Institute, Medical and Biological Laboratories Company Ltd., Terasawaoka, Ina 396-0002, Japan, [6]Tsukuba Primate Center for Medical Sciences, National Institute for Infectious Diseases, Hachimandai, Tsukuba 305-0843, Japan, [7]Graduate School of Pharmaceutical Sciences, Kyoto University, Kyoto 606-8501, Japan, and [8]Center for Neurologic Diseases, Harvard Medical School and Brigham and Women's Hospital, Boston, Massachusetts 02115

A fundamental question about the early pathogenesis of Alzheimer's disease (AD) concerns how toxic aggregates of amyloid β protein (Aβ) are formed from its nontoxic soluble form. We hypothesized previously that GM1 ganglioside-bound Aβ (GAβ) is involved in the process. We now examined this possibility using a novel monoclonal antibody raised against GAβ purified from an AD brain. Here, we report that GAβ has a conformation distinct from that of soluble Aβ and initiates Aβ aggregation by acting as a seed. Furthermore, GAβ generation in the brain was validated by both immunohistochemical and immunoprecipitation studies. These results imply a mechanism underlying the onset of AD and suggest that an endogenous seed can be a target of therapeutic strategy.

Key words: Alzheimer's disease; amyloid; amyloid β protein; seed; ganglioside; raft

Introduction

The lifelong expression of genetic mutations responsible for familial Alzheimer's disease (AD) appears to induce the formation of neurotoxic aggregates of amyloid β protein (Aβ) by accelerating cellular Aβ generation (Selkoe, 1997). However, there is currently no evidence that Aβ generation is enhanced in sporadic, late-onset AD, the principal form of the disease. Thus, it is reasonable to assume that Aβ aggregation in conventional AD may be induced by unknown posttranslational modification(s) of Aβ and/or by altered clearance mechanisms.

We previously identified a novel Aβ species, characterized by its tight binding to GM1 ganglioside (GM1), in human brains that exhibited early pathological changes associated with AD (Yanagisawa et al., 1995, 1997; Yanagisawa and Ihara, 1998). On the basis of the molecular characteristics of the GM1-bound Aβ (GAβ), including its altered immunoreactivity and a strong tendency to form aggregates of Aβ, we hypothesized that Aβ adopts an altered conformation by binding to GM1 and initiates the aggregation of soluble Aβ by acting as a seed (Yanagisawa et al., 1995, 1997; Yanagisawa and Ihara, 1998). Evidence that supports our hypothesis is growing from *in vitro* studies by our group and other groups (McLaurin and Chakrabartty, 1996; Choo-Smith and Surewicz, 1997; Choo-Smith et al., 1997; McLaurin et al., 1998; Matsuzaki and Horikiri, 1999; Ariga et al., 2001; Kakio et al., 2001, 2002).

In the present study, we directly characterize GAβ at the molecular level using a novel monoclonal antibody raised against GAβ purified from an AD brain with the aim of validating our hypothesis. Here we show that GAβ has a conformation distinct from that of soluble Aβ and initiates Aβ aggregation by acting as a seed. Importantly, we successfully verified GAβ generation in the brain by both immunohistochemical and immunoprecipitation methods.

Materials and Methods

Preparation of seed-free Aβ solutions. Aβ solutions were prepared essentially according to a previous report (Naiki and Gejyo, 1999). Briefly, synthetic Aβ (Aβ40 and Aβ42) (Peptide Institute, Osaka, Japan) was dissolved in 0.02% ammonia solution at 500 μM for Aβ40. Aβ42 was dissolved at 250 μM because it has a higher potential to form aggregates rapidly than Aβ40. To obtain seed-free Aβ solutions, the prepared solutions were centrifuged at 540,000 × *g* for 3 hr using the Optima TL Ultracentrifuge (Beckman Instruments, Fullerton, CA) to remove undissolved peptide aggregates, which can act as preexisting seeds. The supernatant was collected and stored in aliquots at −80°C until use. Immediately before use, the aliquots were thawed and diluted with Tris-buffered saline (TBS) (150 mM NaCl and 10 mM Tris-HCl, pH 7.4). In the present study, we used the seed-free Aβ solutions, except in the preparation of Aβ fibrils used as the seeds (see below).

Received Dec. 26, 2003; revised April 14, 2004; accepted April 15, 2004.

This work was supported by research grants for Brain Research Science from the Ministry of Health and Welfare and the Core Research for Evolutional Science and Technology and by a Grant-in-Aid for Scientific Research on Priority Area (C) from the Ministry of Education, Culture, Sports, Science, and Technology (Japan). We thank Y. Ihara for critically reading this manuscript, A. Kakio for assisting in the supplementary experiment, H. Shimokata for performing the statistical analysis, Y. Hanai for assisting in the preparation of this manuscript, and Takeda Chemical Industries Ltd. for providing the antibodies (BAN052).

Correspondence should be addressed to Dr. Katsuhiko Yanagisawa, Department of Dementia Research, National Institute for Longevity Sciences, 36-3 Gengo, Morioka, Obu, 474-8522, Japan. E-mail: katuhiko@nils.go.jp.

H. Hayashi's present address: Department of Medicine, University of Alberta, Edmonton, T6G 2S2, Canada.

DOI:10.1523/JNEUROSCI.0861-04.2004

 0270-6474/04/244894-09$15.00/0

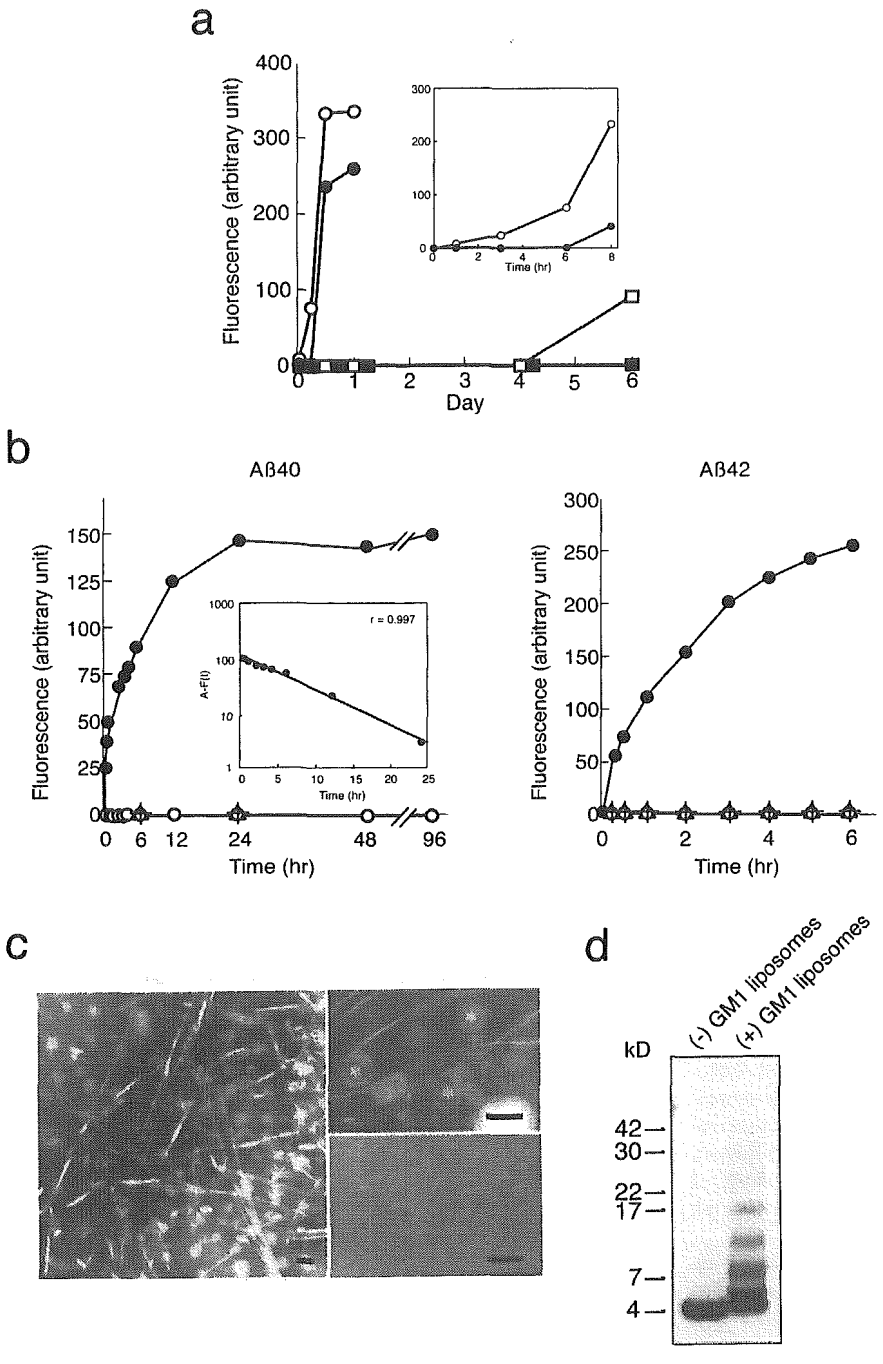

Figure 1. Amyloid fibril formation from soluble Aβ in the absence or presence of GM1-containing liposomes. *a*, Kinetics of Aβ fibrillogenesis using Aβ (Aβ40 and Aβ42) solutions, with or without removing undissolved peptide aggregates, which can act as preexisting seeds. Aβ solutions were incubated at 50 μM and 37°C. Open and filled circles indicate ThT fluorescence intensities of Aβ42 solutions without and with removing undissolved peptide aggregates, respectively. Open and filled squares indicate ThT fluorescence intensities of Aβ40 solutions without and with removing undissolved peptide aggregates, respectively. *b*, Kinetics of Aβ fibrillogenesis. Aβ (Aβ40 and Aβ42) solutions, after removal of undissolved peptide aggregates, were incubated at 50 μM and 37°C in the presence of GM1-containing liposomes (filled circles) or GM1-lacking liposomes (plus signs) or were incubated in the absence of liposomes (open circles). The GM1-containing liposomes alone were also incubated in the absence of Aβ (triangles). The fluorescence intensity of thioflavin T was obtained by excluding background activity at 0 hr. Inset, Semilogarithmic plot of the difference, $A - F(t)$, versus incubation time (0–24 hr). $F(t)$ represents the increase in fluorescence intensity as a function of time in the case of Aβ incubated with GM1-containing liposomes, and A is tentatively determined as F (infinity). Linear regression and correlation coefficient values were calculated ($r = 0.997$). $F(t)$ is described by a differential equation: $F'(t) = B - CF(t)$. *c*, Electron micrographs of the Aβ40 solutions incubated at 50 μM and 37°C for 24 hr with GM1-containing liposomes (left and right top panels) or without liposomes (right bottom panel). The liposomes are indicated by asterisks. Scale bars, 50 nm. *d*, Western blot of Aβ40 solutions incubated at 50 μM and 37°C for 24 hr in the presence or absence of GM1-containing liposomes. The incubated Aβ solutions were centrifuged at 100,000 × *g* for 15 min. Ten nanograms of Aβ in the supernatant were subjected to SDS-PAGE (4–20%) after glutaraldehyde treatment. The Aβ in the gel was detected by Western blotting using BAN052. Aβ oligomers were detected in the Aβ solution incubated in the presence of GM1-containing liposomes but not detected in the incubation mixture containing Aβ alone.

Preparation of Aβ40 seeds. Aβ40 fibrils used as exogenous seeds were prepared essentially according to the method reported previously (Naiki and Nakakuki, 1996). Briefly, Aβ40 solution was incubated at 500 μM and 37°C for 72 hr without previous removal of the preexisting seeds. After incubation, newly formed Aβ40 fibrils were precipitated by ultracentrifugation. The resultant pellets were subjected to sonication. Protein concentrations of the solutions containing Aβ40 fibrils were determined using a protein assay kit (Bio-Rad, Hercules, CA) as described previously (Bradford, 1976). The Aβ40 solution quantified by amino acid analysis was used as the standard. Aliquots of the solution were stored at −80°C until use.

Preparation of liposomes. Cholesterol and sphingomyelin (Sigma, St. Louis, MO) and GM1 (Wako, Osaka, Japan) were dissolved in chloroform/methanol (1:1) at a molar lipid ratio of 2:2:1 to generate GM1-containing liposomes. GM1-lacking liposomes were prepared by mixing cholesterol and sphingomyelin at a molar lipid ratio of 1:1. The mixtures were stored at −80°C until use. Immediately before use, the lipids were resuspended in TBS at a GM1 concentration of 2.5 mM and subjected to freezing and thawing. The lipid suspension was centrifuged once at 15,000 × *g* for 15 min, and the resultant pellet was resuspended in TBS. Finally, the suspension was subjected to sonication on ice.

Thioflavin T assay. The assay was performed according to a method described previously (Naiki and Gejyo, 1999) on a spectrofluorophotometer (RF-5300PC; Shimadzu, Tokyo, Japan). Optimum fluorescence measurements of amyloid fibrils were obtained at the excitation and emission wavelength of 446 and 490 nm, respectively, with the reaction mixture (1.0 ml) containing 5 μM thioflavin T (ThT) (Sigma) and 50 mM glycine-NaOH buffer, pH 8.5. Fluorescence was measured immediately after making the mixture. The Aβ (Aβ40 and Aβ42) solution described above was incubated at 37°C with liposomes at an Aβ concentration of 50 μM at a GM1/Aβ molar ratio of 10:1.

Detection of Aβ oligomers by SDS-PAGE. The Aβ40 solution described above was incubated with liposomes at an Aβ concentration of 50 μM at a GM1/Aβ molar ratio of 10:1 for 24 hr at 37°C and then centrifuged at 100,000 × *g* for 15 min. The supernatant was subjected to SDS-PAGE after glutaraldehyde treatment (LeVine, 1995) to stabilize oligomeric Aβ during SDS-PAGE. The Aβ in the gel was detected by Western blotting using BAN052, a monoclonal antibody specific to the N terminus of Aβ (Suzuki et al., 1994), as reported previously (Yanagisawa et al., 1995).

Experiments using animal models. All experiments using animals were performed in compliance with existing laws and institutional guidelines. For experiments using nonhuman primates, animals were anesthetized with pentobarbital (25 mg/kg, i.p.) and killed by draining blood from the heart.

Cell culture. Cerebral cortical neuronal cultures were prepared from Sprague Dawley rats

at embryonic day 17 as described previously (Michikawa and Yanagisawa, 1998). The dissociated single cells were suspended in a feeding medium and plated onto poly-D-lysine-coated 12-well plates at a cell density of 2.5×10^5/well. The feeding medium, N2, consisted of DMEM–F-12 containing 0.1% bovine serum albumin fraction V solution (Invitrogen, Gaithersburg, MD) and N2 supplements. The reagents examined, including TBS, Aβ40, GM1-lacking liposome, and GM1-containing liposome in the absence or presence of Aβ40, were prepared as described above. For treatment, at 24 hr after plating, the culture medium was changed with fresh N2 medium diluted with the same volume of each reagent solution. At 48 hr after the commencement of the treatment, phase-contrast photomicrographs of each culture were taken, and the cells were stained with propidium iodide, which selectively permeates the broken membranes of dying cells and stains their nuclei, and with a viable cell-specific marker, calcein AM, as described previously (Michikawa and Yanagisawa, 1998). Photomicrographs were taken by laser confocal microscopy (Zeiss, Oberkochen, Germany) and the number of viable neurons on each micrograph was determined in each microscope field (40× objective). Two hundred to 500 cells were counted for each determination of cell viability. Statistical analysis was performed using ANOVA.

Production of 4396C. The IgG monoclonal antibody 4396C was produced by the genetical class-switch technique (Binding and Jones, 1996) from IgM hybridomas that were raised against GAβ purified from an AD brain. The procedures for the generation and characterization of the original IgM monoclonal antibody 4396 were reported previously (Yanagisawa et al., 1997).

Immunoelectron microscopy. GM1-containing and GM1-lacking liposomes were mixed with soluble Aβ40 on ice for 5 sec at a weight ratio of lipid/Aβ40 at 100:3. The mixtures were immediately ultracentrifuged to remove unbound Aβ40, and liposome pellets were fixed for immunoelectron microscopy of 4396C or isotype-matched control IgG staining. They were then incubated with gold-tagged goat anti-mouse IgG. Aβ40 fibrils formed by the extension reaction of Aβ40 seeds (10 μg/ml) with seed-free Aβ40 (50 μM) as described above, were also subjected to immunoelectron microscopy of 4396C, isotype-matched control IgG, or 4G8 (Kim et al., 1988) staining. The first antibodies and control IgG were diluted at 1:100 using PBS containing 1% bovine serum albumin (PBS-BSA).

Quantitative binding assay. GM1-containing liposomes and GM1-lacking liposomes were mixed with soluble Aβ40 at various concentrations (2.5–25 μM) by vortexing for 60 sec, and the mixtures were ultracentrifuged at 540,000 × *g* for 10 min to remove unbound Aβ40. Then, 4396C and isotype-matched control IgG, at a concentration of 10 μg/ml in PBS-BSA, were incubated with the liposomes at room temperature for 60 min. After incubation, the mixtures were ultracentrifuged at 540,000 × *g* for 20 min, and the resultant pellets were washed with PBS-BSA to remove the unbound antibody. The levels of IgG bound to the liposomes were determined after the incubation of liposomes with peroxidase-conjugated goat anti-mouse IgG using cyanogen bromide Sepharose CL4B-bound 4396C as the standard.

Dot blot analysis. Liposomes carrying GAβ were prepared by mixing GM1-containing liposomes with soluble Aβ (Aβ40 and Aβ42) on ice for 5 sec at a weight ratio of lipid/Aβ at 100:3. The liposomes, and Aβ and GM1, in amounts equal to those contained in blotted liposomes (300 and 600 ng of Aβ; 2 and 4 μg of GM1), were blotted. The blots were incubated with 4396C (1:1000), BAN052 (1:5000), HRP-conjugated cholera toxin subunit B (CTX) (1:20,000), or the isotype-matched control IgG (1:1000). The blots incubated with 4396C, BAN052, or control IgG were then incubated with horseradish peroxidase-conjugated anti-mouse IgG (Invitrogen). The bound-enzyme activities were visualized with an ECL system (Amersham Biosciences, Buckinghamshire, UK).

Inhibition assay of Aβ aggregation. Soluble Aβ40 (50 μM) was incubated at 37°C with GM1-containing liposomes (GM1/Aβ molar ratio of 10:1) or preformed Aβ40 seeds (10 μg/ml), which were prepared as described above, and an antibody (4396C or 4G8) at various concentrations. Aβ40 aggregation levels in the mixtures were determined by ThT assay.

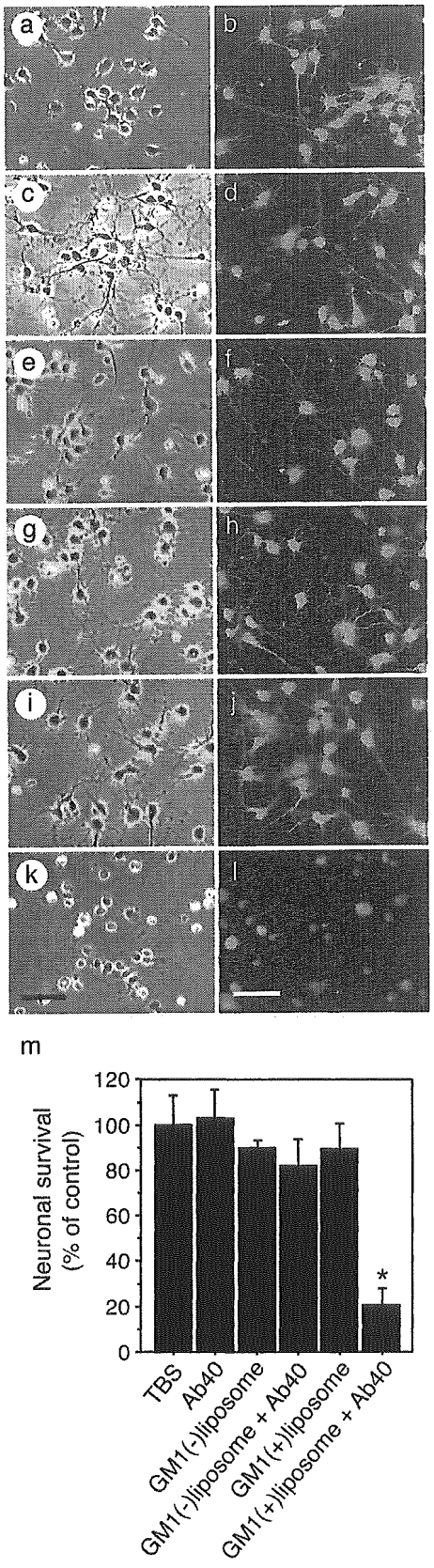

Figure 2. Viability of neurons treated with Aβ40 incubated in the presence of GM1 ganglioside. Phase-contrast and calsein AM– ethidium homodimer-stained photographs of cultured neurons were taken after treatment with TBS (*a*, *b*), Aβ40 (*c*, *d*), GM1-lacking liposomes (*e*, *f*), GM1-lacking liposomes plus Aβ40 (*g*, *h*), GM1-containing liposomes (*i*, *j*), and GM1-containing liposomes plus Aβ40 (*k*, *l*). *m*, Viable cells stained with calcein AM were counted. The data represent means ± SE for triplicate samples. *$p < 0.003$ versus other treatments. Scale bars, 20 μm.

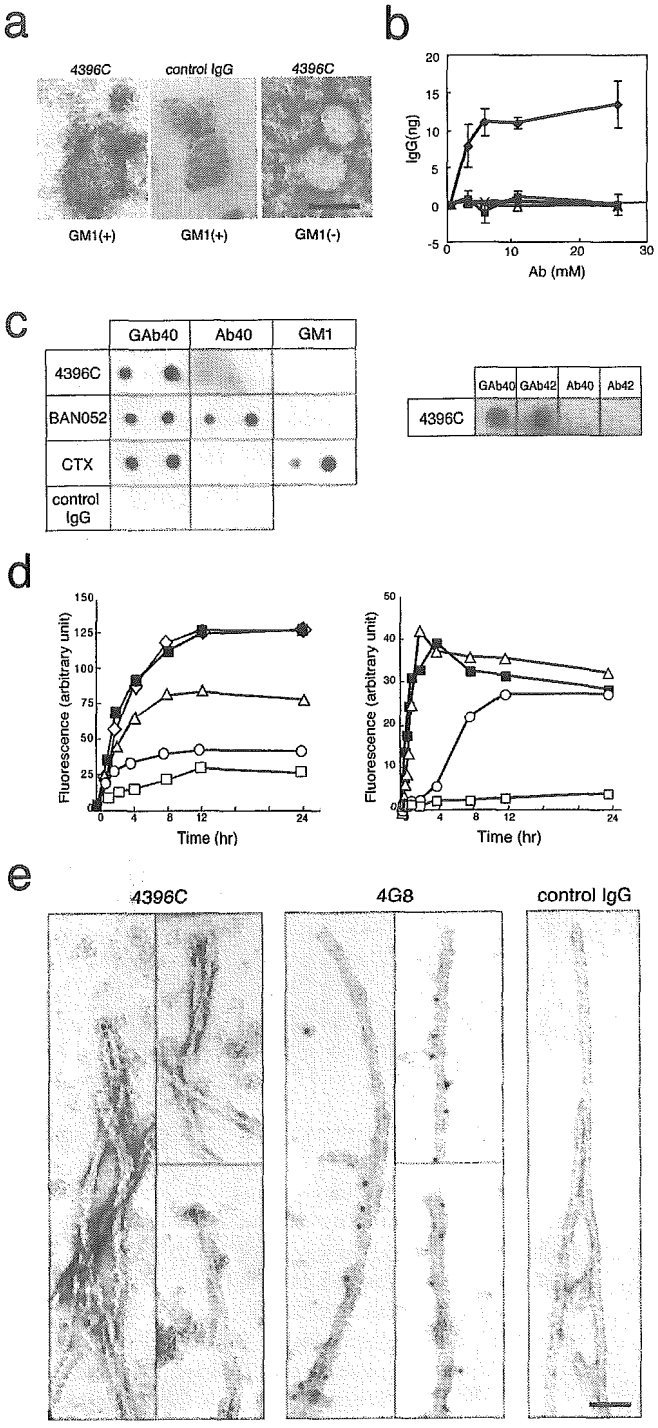

Figure 3. Characterization of the binding specificity of 4396C. *a*, Immunoelectron micrographs of liposomes. GM1-containing and GM1-lacking liposomes were subjected to immunoelectron microscopy of 4396C or isotype-matched control IgG staining after incubation with soluble Aβ40. GM1(+), GM1-containing liposomes; GM1(−), GM1-lacking liposomes. Scale bar, 50 nm. *b*, Quantitative assay of binding of 4396C to liposomes. GM1-containing liposomes were incubated with 4396C (diamonds) or isotype-matched control IgG (filled squares) after their mixing with soluble Aβ40 at indicated concentrations. GM1-lacking liposomes were also incubated with 4396C (triangles) or isotype-matched control IgG (× symbols). Ab, Antibody. *c*, Dot blot analysis. Left, Liposomes carrying GAβ (GAβ40), Aβ40, and GM1 in amounts equal to those contained in blotted liposomes (300 and 600 ng of Aβ40; 2 and 4 μg of GM1) were blotted. The blots were incubated with 4396C, BAN052, HRP-conjugated CTX, or isotype-matched control IgG. Right, Liposomes carrying GAβ (GAβ40 and GAβ42), prepared using Aβ40 or Aβ42, and Aβ40 and Aβ42 in amounts equal to those contained in GAβ40 and GAβ42 (600 ng of each peptide) were blotted. The blots were incubated with 4396C. *d*, Inhibition of amyloid fibril formation from soluble Aβ40 by 4396C. Left, Soluble Aβ40 was incubated with GM1-containing liposomes in the absence (filled squares) or presence of an antibody (4396C or 4G8). The molar ratios of 4396C to soluble Aβ40 were 0.3:50 (triangles), 1.3:50 (circles), and 4:50 (open squares) and that of 4G8 to Aβ40 was 4:50 (diamonds). Right, Soluble Aβ40 was incubated with preformed Aβ40 fibrils in the absence of an antibody (filled squares) or in the presence of 4396C. The molar ratios of 4396C to soluble Aβ40 were 0.3:50 (triangles), 1.3:50 (circles), and 4:50 (open squares). *e*, Immunoelectron micrographs of preformed Aβ40 fibrils. Aβ40 fibrils were formed by the extension reaction of Aβ40 seeds (10 μg/ml) with seed-free Aβ40 (50 μM), as described in Materials and Methods, and subjected to immunoelectron microscopy of 4396C, 4G8, or isotype-matched control IgG staining. Scale bar, 50 nm.

Immunohistochemistry. Sections of cerebral cortices of human brains, which were fixed in 4% formaldehyde or Kryofix (Merck, Darmstadt, Germany) and embedded in paraffin, were immunolabeled with 4396C (10 μg/ml) or 4G8 (1 μg/ml) after pretreatment with formic acid (99%) or SDS (4%). Sections of cerebral cortices of nonhuman primates at various ages (4, 5, 17, 19, 20, 30, and 36 years old) were fixed with 1% paraformaldehyde and subjected to immunohistochemistry with 4396C (10 μg/ml). For double staining with 4396C and BAN052, we first labeled 4396C with FITC to distinguish its reaction from that of BAN052. The binding of BAN052 was detected using Alexa 568-conjugated anti-mouse IgG (Molecular Probes, Eugene, OR). For double staining with 4396C and CTX, we used a zenon one-mouse IgG2a labeling kit (Molecular Probes) for the previous conjugation of 4396C with Alexa 568. For GM1 detection, we used FITC-conjugated cholera toxin subunit B (Sigma). Autofluorescence was blocked by pretreatment with Sudan Black B (Tokyo Kasei Kogyo Company, Tokyo, Japan).

Immunoprecipitation. Immunoprecipitation of GAβ from nonhuman primate brains was performed as described previously (Yanagisawa and Ihara, 1998). Briefly, cerebral cortices of primates were Dounce homogenized with 9 vol of TBS, pH 7.6. Homogenates were subjected to sucrose density gradient fractionation to obtain the membrane fraction. The membrane fraction was dried and then directly labeled with 4396C (5 μg/ml) after sonication on ice. After 1 hr incubation, the mixtures were centrifuged at 15,000 × *g* for 10 min to remove the unbound antibody. The pellets were washed with TBS and solubilized in radioimmunoprecipitation assay buffer (0.1% SDS, 0.5% deoxycholic acid, and 1% NP-40) for 5 min and then centrifuged at 15,000 × *g* for 10 min. Supernatants were collected and diluted with TBS. Protein G Sepharose (PGS) (Amersham Biosciences, Piscataway, NJ), which had been precoated with goat anti-mouse IgG, was added to the supernatants. Finally, PGS pellets were thoroughly washed with TBS containing 0.05% Tween 20.

Results

Kinetics of Aβ fibrillogenesis in the presence of GM1 ganglioside

As reported previously (Naiki et al., 1998; Ding and Harper, 1999), the removal of preexisting seeds is critical in the kinetic study of Aβ fibril formation *in vitro*. The ThT fluorescence intensity of Aβ42 solutions without removing undissolved peptide aggregates, which can act as preexisting seeds, started to increase as early as 1 hr of incubation at 50 μM and 37°C (Fig. 1*a*). In contrast, the ThT fluorescence intensity of seed-free Aβ42 solutions did not increase as long as 6 hr of incubation under the same conditions (Fig. 1*a*). The ThT fluorescence intensity of Aβ40 solutions without removing undissolved peptide aggregates started to increase after 4 d of incubation at 50 μM and 37°C (Fig. 1*a*); however, the seed-free Aβ40 solutions incubated under the same conditions did not show any increase in the ThT fluorescence intensity at this point (Fig. 1*a*). Thus, to investigate the molecular process of GAβ-initiated Aβ aggregation, we incubated the seed-free Aβ (Aβ40 and Aβ42) solutions at 50 μM and 37°C under various conditions, as long as 48 and 6 hr for Aβ40 and Aβ42, respectively, in the following experiments.

We incubated Aβ40 solutions in the presence or absence of GM1-containing liposomes. The ThT fluorescence intensity in-

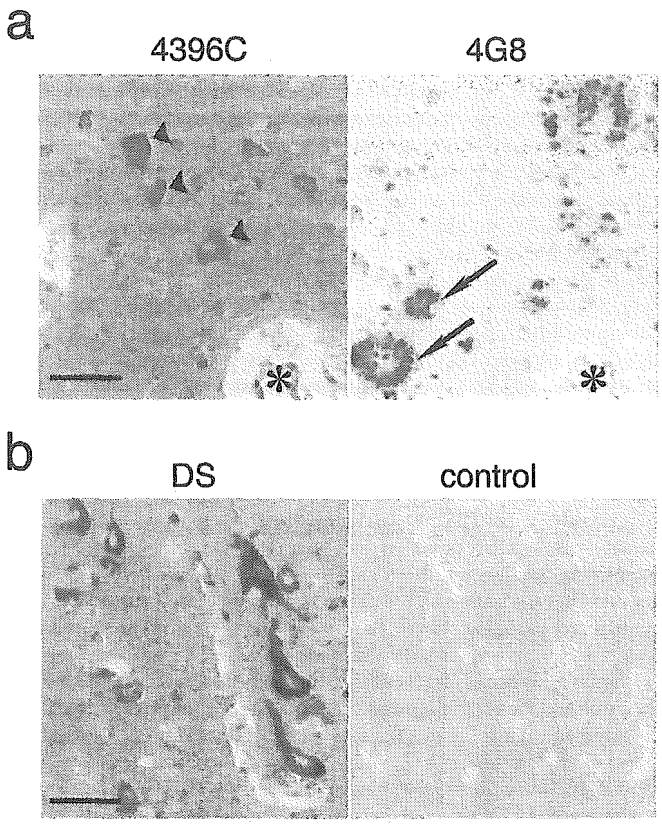

Figure 4. Immunohistochemistry of GAβ in sections of human brains. *a*, Immunostaining of serial sections of the cerebral cortex of an AD brain fixed in Kryofix and pretreated with SDS. Neurons (arrowheads) were immunostained by 4396C but not by 4G8, whereas plaques (arrows) were immunostained by 4G8 but not by 4396C. The asterisks indicate the same blood vessel in the serial sections. Scale bar, 50 μm. *b*, Immunostaining by 4396C of sections of cerebral cortices of DS (left) and control (right) brains fixed in Kryofix and pretreated with SDS (DS, 47 years old; control, 65 years old). Scale bar, 50 μm.

Table 1. Neuronal immunoreactivity to 4396C in human cerebral cortices

	Score				
	0	1	2	3	4
Control (22)	4	5	12	1	0
AD (5)	0	2	2	1	0
DS (2)	0	0	0	0	2

Intensities of neuronal immunoreactivity to 4396C were semiquantitatively assessed in cerebral cortices obtained from nondemented individuals (Control), patients with AD, and those with DS. The numbers in parentheses indicate the number of cases. 0, Absent; 1, weak; 2, moderate; 3, intense; 4, most intense. Difference in the neuronal immunoreactivities between control and AD plus DS was significant ($p < 0.05$, Mentel-Haenszel χ^2 test; $p < 0.05$, Cochran-Armitage trend test).

creased without a lag phase after the addition of GM1-containing liposomes to the Aβ40 solutions (Fig. 1*b*). In contrast, there was no increase in the ThT fluorescence intensity of the solutions containing Aβ40 alone or Aβ40 plus GM1-lacking liposomes during an incubation period of as long as 96 hr (Fig. 1*b*). By a semilogarithmic calculation, a perfect linear plot ($r = 0.997$) was obtained for the experiment using GM1-containing liposomes (Fig. 1*b*, inset). The fluorescence intensity of ThT also increased in seed-free Aβ42 solution after the addition of GM1-containing liposomes (Fig. 1*b*). Under an electron microscope, typical amyloid fibrils were observed in the Aβ40 solution after 24 hr incubation at 50 μM and 37°C in the presence of GM1-containing liposomes (Fig. 1*c*). These results suggest that Aβ binds to GM1, leading to the generation of GAβ, and then induces Aβ fibrillogenesis in the manner of a first-order kinetic model (Naiki and Nakakuki, 1996) by acting as a seed; that is, the extension of fibrils is likely to proceed via consecutive binding of soluble Aβ first onto GAβ and then onto the ends of growing fibrils.

We then investigated whether the formation of Aβ oligomers is also acclerated in the presence of GM1 ganglioside. We perfomed SDS-PAGE of the Aβ40 solutions incubated at 50 μM and 37°C for 24 hr. Notably, Aβ oligomers were detected by Western blotting of the SDS-PAGE in the incubation mixture with GM1-containing liposomes but was not detected in the incubation mixture containing Aβ40 alone (Fig. 1*d*).

Neurotoxicity of Aβ incubated in the presence of GM1 ganglioside

We then investigated whether Aβ aggregates formed in the presence of GM1-containing liposomes are neurotoxic. We incubated Aβ40 solutions in the presence or absence of GM1-containing liposomes for 24 hr and then applied them to a primary neuronal culture after dilution with N2 media. In this experiment conducted 48 hr after the commencement of the treatment, significant neuronal death was observed only in the culture treated with the Aβ40 solution incubated in the presence of GM1-containing liposomes (Fig. 2).

Molecular characterization of GAβ

To characterize GAβ at the molecular level and to clarify the process of Aβ aggregation in the presence of GM1, we raised a monoclonal antibody against natural GAβ purified from an AD brain. In an experiment using immunoelectron microscopy, the antibody (4396C), but not the isotype-matched control IgG, recognized artificially generated GAβ on liposomes (Fig. 3*a*). The specificity of 4396C to GAβ was confirmed by quantitative binding assay (Fig. 3*b*) and dot blot analysis (Fig. 3*c*, left). Notably, 4396C did not recognize the unbound forms of Aβ40 and GM1, whereas BAN052, a monoclonal antibody specific to the N terminus of Aβ (Suzuki et al., 1994), recognized both GAβ40 and Aβ (Fig. 3*c*, left). The 4396C antibody reacted with GM1-bound forms of two Aβ isoforms (Aβ40 and Aβ42) (Fig. 3*c*, right). In the inhibition assay of Aβ fibrillogenesis, the increase in the fluorescence intensity of ThT of the Aβ40 plus GM1-containing liposomes was suppressed by 4396C in a dose-dependent manner (Fig. 3*d*, left). In contrast, the increase in the fluorescence intensity of ThT was not affected by 4G8, a monoclonal antibody specific to amino acid residues 17–24 of Aβ (Kim et al., 1988) (Fig. 3*d*, left). We then examined the possibility that Aβ fibrillogenesis proceeds with consecutive conformational alteration of Aβ at the ends of growing fibrils; that is, GAβ and Aβ at the ends of growing fibrils share a specific conformation that is required for Aβ fibrillogenesis in the manner of a first-order kinetic model. We incubated Aβ40 solutions with 4396C in the presence of preformed Aβ40 seeds instead of GM1-containing liposomes. Notably, 4396C inhibited the increase in the fluorescence intensity of ThT under this condition in a dose-dependent manner (Fig. 3*d*, right). To further examine this possibility, we performed immunoelectron microscopy using preformed Aβ40 fibrils. In this experiment, 4396C bound only to the ends but not to the lateral sides of the fibrils, whereas 4G8 bound only to the lateral sides (Fig. 3*e*).

GAβ generation in the brain

Having established the specificity of 4396C, we then aimed to detect GAβ in the brain by immunohistochemistry. We first performed routine immunohistochemistry: that is, fixation in formaldehyde and enhancement of immunoreactivity by formic acid

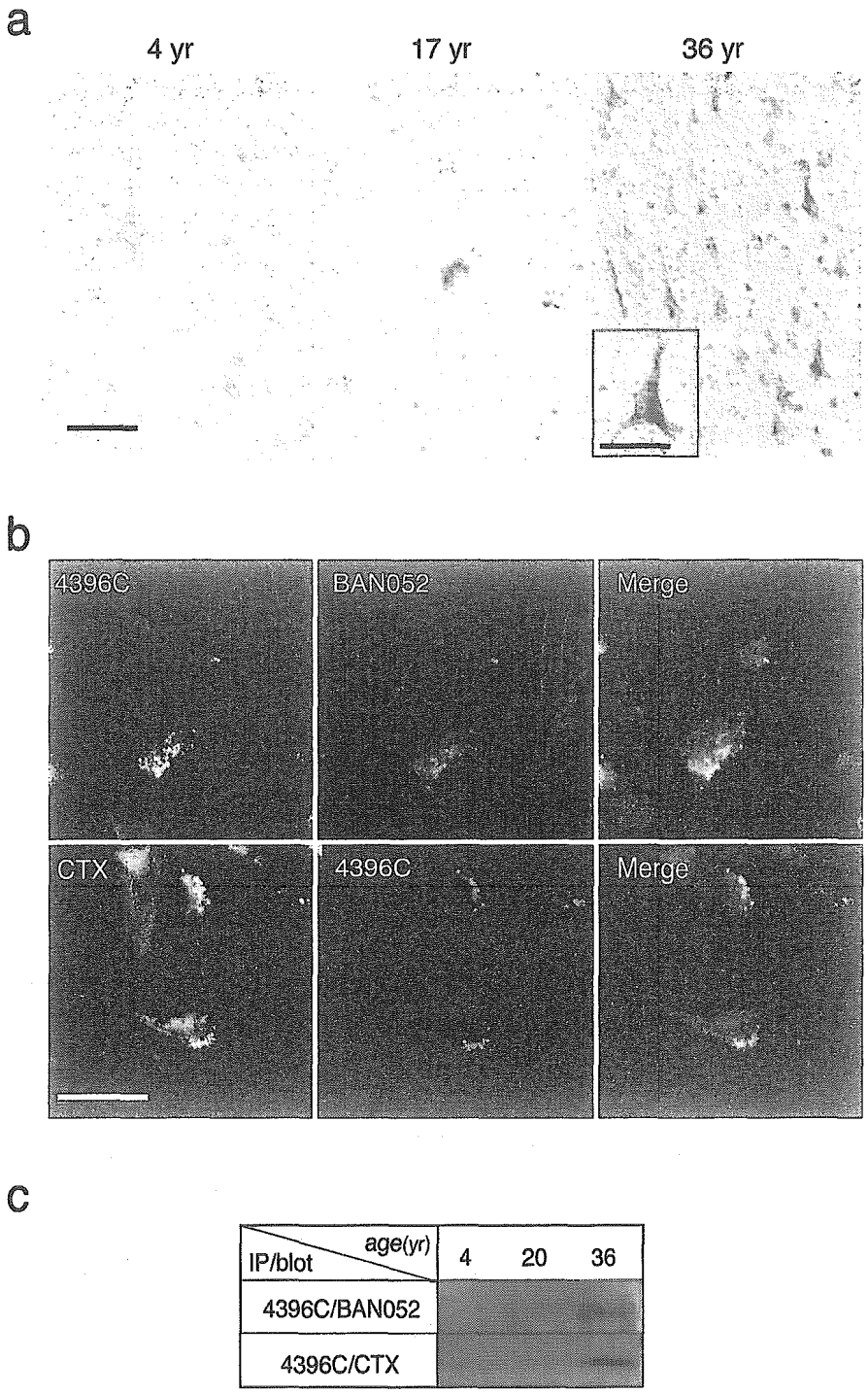

Figure 5. Immunohistochemistry and immunoprecipitation of GAβ in sections of nonhuman primate brains. *a*, Immunostaining by 4396C of sections of the cerebral cortices of primate brains, which were fixed in paraformaldehyde, from animals of different ages. Scale bar, 50 μm. Inset, Higher magnification. Scale bar, 20 μm. *b*, Double immunostaining of sections of the cerebral cortex of a 36-year-old primate brain, which was fixed in paraformaldehyde, after the blocking of autofluorescence by pretreatment with Sudan Black B. Colocalization of immunostaining by 4396C and that by BAN052 or CTX is shown in the merged image. Scale bar, 25 μm. *c*, Immunoprecipitation of GAβ by 4396C from cerebral cortices of primates at different ages. Immunoprecipitates were blotted and reacted with BAN052 or HRP-conjugated CTX.

or microwave treatment of brain sections. Under these conditions, no immunostaining by 4396C was observed in AD brains (data not shown), suggesting that the conformation of GAβ is sensitive to the procedures of conventional immunohistochemistry. Thus, we used an alternative fixation procedure using Kryofix, because it eliminates the possibility of obtaining false-negative results that usually occur when using formaldehyde-fixed sections (Boon and Kok, 1991), and we also pretreated sections with SDS, which is known to improve immunostaining (Barrett et al., 1999). With these procedures, neurons in the cerebral cortices of AD brains were immunostained by 4396C (Fig. 4*a*). Although neuropil staining was rather strong, plaques were not recognized by 4396C (Fig. 4*a*). In contrast to staining by 4396C, 4G8 immunostained plaques but did not react with neurons (Fig. 4*a*). We performed immunohistochemistry of cerebral cortices of 22 nondemented control individuals (36–91 years old), which included one amyotrophic lateral sclerosis patient (44 years old) and two Down's syndrome (DS) patients (47 and 52 years old), in addition to five AD patients (65–96 years old). The most intense neuronal staining by 4396C was observed in the brains of both DS patients (Fig. 4*b*). In the sections of control brains, neuronal staining was absent (Fig. 4*b*) or at comparable levels with those of AD brains (Table 1). These results suggest that GAβ can be detected by immunohistochemistry, but neuronal staining by 4396C under these conditions can also be nonspecifically induced, probably because of changes that occur during the agonal and/or postmortem state. Thus, to confirm the immunohistochemical detection of GAβ, we then examined fresh nonhuman primate (*Macaca fascicularis*) brains, which naturally and consistently develop Aβ deposition at ages >25 years (Nakamura et al., 1998). Cerebral cortices of seven animals at different ages (4, 4, 5, 17, 19, 30, and 36 years old) were fixed with paraformaldehyde, because it also preserves tissue and cell surface antigens (Smit et al., 1974), and were subjected to 4396C immunostaining without pretreatment with SDS. In the sections obtained from the two older animals, that is, 30 years old (data not shown) and 36 years old (Fig. 5*a*), a number of neurons were strongly immunostained by 4396C with a granular pattern (Fig. 5*a*, inset). In these sections, plaques were immunostained by 4G8 but not by 4396C (data not shown). In the sections of cerebral cortices of the five animals at ages <20 years old, which showed no plaques, the neuronal staining by 4396C was generally at negligible levels, and the strong staining was only occasionally observed in the sections from the 17-year-old (Fig. 5*a*) and 19-year-old (data not shown) animals. In double immunostaining of the sections obtained from the 36-year-old animal, intraneuronal staining by 4396C was distinctly colocalized with that by BAN052 or cholera toxin, a natural ligand specific to GM1 (Fig. 5*b*). To verify GAβ generation in the brain, we performed an

immunoprecipitation study using 4396C. GAβ was immunoprecipitated by 4396C only from the cerebral cortex of the older animal (Fig. 5*c*). These results indicate that GAβ is generated in the brain.

Discussion

In regard to the formation of pathogenic aggregates of constituent proteins, including Aβ and prion proteins, the seeded polymerization theory was proposed previously (Harper and Lansbury, 1997). For the transition of the nontoxic monomeric form of Aβ to its toxic aggregated form, the template-dependent dock-lock mechanism was reported previously (Esler et al., 2000). The present study supports these possibilities and also indicates that a seed can be endogenously generated by the binding of an aggregating protein to another molecule as was suggested in the mechanism underlying the aggregation of prion proteins (Telling et al., 1995; Deleault et al., 2003).

To understand the early events in the development of AD and also to develop tharapeutic strategies, clarification of the time course of Aβ fibrillogenesis is fundamentally important. Previously, Harper et al. analyzed the process of *in vitro* Aβ assembly using an atomic force microscope at a fine resolution. They reported that protofibrils, transient species of Aβ assembly, are formed during the first week of incubation of Aβ40 before mature fibrils are generated (Harper et al., 1997a,b, 1999; Ding and Harper, 1999). This model of Aβ assembly was supported by a recent study of Nichols et al. (2002). In the present study, we examined the acceleration of Aβ aggregation in the presence of GM1 ganglioside. In the EM examination of the present study, we observed mature fibrils in Aβ40 solutions incubated at 50 μM and 37°C for 24 hr, but protofibrils were hardly recognized (Fig. 1*c*). This discrepancy is likely to mainly stem from the presence or absence of GM1-containing liposomes and the differences in incubation period and peptide concentrations. Additional careful examination at a much greater resolution is required; however, the molecular process of Aβ fibrillogenesis in the presence of GM1 ganglioside may be different from that initiated by spontaneous nucleation from seed-free Aβ solution.

From the results of molecular characterization of GAβ in the present study, it seems likely that Aβ adopts an altered conformation at its midportion through binding to GM1 because GAβ was readily recognized by BAN052, an antibody specific to the N terminus of Aβ, and 4396C comparably recognized two Aβ isoforms with different lengths at their C termini. This possibility is supported by the following: first, 4G8, an antibody specific to the midportion of Aβ, failed to react with GAβ in the inhibition assay of Aβ aggregation; and second, BAN052, but not 4G8, immunoprecipitated GAβ from the cerebral cortex of an AD brain in our previous study (Yanagisawa and Ihara, 1998). The conformational epitope for 4396C on the Aβ molecule remains to be determined; however, the results of the present study suggest that the 4396C-reactive conformation, which is shared by GAβ and Aβ at the ends of fibrils, is necessary for Aβ fibrillogenesis. Because amyloid fibrils composed of various proteins share a common structure that is readily recognized by Congo red, it may be interesting to study in the future whether the 4396C-reactive conformation is shared by seed or oligomer of other amyloidogenic proteins. Regarding this, we must draw attention to a recent report by Glabe and his colleagues (Kayed et al., 2003): they have successfully generated an antibody that potentially recognizes the common structure of soluble amyloid oligomers. Their results suggest that the oligomers have a conformation that is distinct from those of soluble monomers and amyloid fibrils.

In this study, only careful immunohistochemistry allowed us to visualize seed molecules, suggesting that we may likely fail to detect some population of seed molecules unless their conformations are preserved during immunohistochemistry. This may also be the case with other neurodegenerative diseases in which seed molecules are likely to play a critical role in the initiation of aggregation of soluble proteins. In this study, it remains to be clarified why 4396C did not immunostain plaques in which the ends of amyloid fibrils were supposed to exist. Possible explanations for this failure are as follows; first, the number of epitopes that can be recognized by the antibody may be limited, as was clearly indicated by immunoelectron microscopy using fibrils; second, we may have lost their immunoreactivities because of their higher susceptibility to treatment in immunohistochemistry than GAβ; and third, the ends of amyloid fibrils may have been masked or modified in the brain (Shapira et al., 1988; Roher et al., 1993).

A challenging subject of studies in the future is determining how and where GAβ is generated in the brain. Regarding this issue, we favor the possibility that GAβ is generated in GM1- and cholesterol-rich microdomains such as lipid rafts (Parton, 1994; Simons and Ikonen, 1997), because of the following: (1) lipid rafts contain soluble and insoluble Aβs under physiological (Lee et al., 1998; Morishima-Kawashima and Ihara, 1998) and pathological (Sawamura et al., 2000) conditions, respectively; (2) amyloidogenic processing of the amyloid precursor protein is associated with lipid rafts (Ehehalt et al., 2003); and (3) the aggregation of soluble Aβ is readily induced by its interaction with lipid raft-like model membranes (Kakio et al., 2003). We found recently that Aβ binding to GM1 is markedly accelerated in a cholesterol-rich environment and that, in such an environment, GM1 forms a cluster that can be recognized by soluble Aβ as a receptor (Kakio et al., 2001). The alteration of cholesterol content in the AD brain is a controversial issue; however, it is noteworthy that cholesterol content in the outer leaflet of the synaptic plasma membrane can be increased in association with risk factors for the development of AD, including aging (Igbavboa et al., 1996) and the expression of apolipoprotein E allele ε4 (Hayashi et al., 2002). Thus, altogether, one possible scenario may be as follows: GAβ is generated in the lipid rafts or lipid raft-like microdomains in the neuron because of an increase in the local concentration of cholesterol, and then, GAβ initiates its seed activity to accelerate Aβ aggregation after its transport to the neuronal surface and/or shedding into the extracellular space. Alternatively, GAβ itself can be noxious per se because it has been reported previously that the disruption of membranes (McLaurin and Chakrabartty, 1996) and alteration of bilayer organization (Matsuzaki and Horikiri, 1999) can be induced by the generation of GAβ on the membranes. Thus, it may also be worthy to examine in future studies whether GAβ causes impairment of neuronal, particularly lipid raft-related, functions before extraneuronal Aβ deposition.

Several studies have suggested that therapeutically useful antibodies can be generated (Solomon et al., 1997; Bard et al., 2000; Hock et al., 2002; McLaurin et al., 2002; Lombardo et al., 2003). Together with the finding that GAβ has a conformation distinct from that of soluble Aβ, it may be possible to develop a novel therapeutic strategy to specifically inhibit the initiation of oligomerization–polymerization of Aβ in the brain.

References

Ariga T, Kobayashi K, Hasegawa A, Kiso M, Ishida H, Miyatake T (2001) Characterization of high-affinity binding between gangliosides and amyloid beta-protein. Arch Biochem Biophys 388:225–230.

Bard F, Cannon C, Barbour R, Burke RL, Games D, Grajeda H, Guido T, Hu K, Huang J, Johnson-Wood K, Khan K, Kholodenko D, Lee M, Lieberburg I, Motter R, Nguyen M, Soriano F, Vasquez N, Weiss K, Welch B, et al. (2000) Peripherally administered antibodies against amyloid beta-peptide enter the central nervous system and reduce pathology in a mouse model of Alzheimer disease. Nat Med 6:916–919.

Barrett JE, Wells DC, Conrad GW (1999) Pretreatment methods to improve nerve immunostaining in corneas from long-term fixed embryonic quail eyes. J Neurosci Methods 92:161–168.

Binding MM, Jones ST (1996) Rodent to human antibodies by CDR grafting. In: Antibody engineering (Mcmafferty J, Hoogenboon HR, Chiswell DJ, eds), pp 147–168. Oxford: Oxford UP.

Boon ME, Kok LP (1991) Formalin is deleterious to cytoskeleton proteins: do we need to replace it by formalin-free Kryofix? Eur J Morphol 29:173–180.

Bradford MM (1976) A rapid and sensitive method for the quantitaion of microgram quantities of protein utilizing the principle of protein-dye binding. Anal Biochem 72:248–254.

Choo-Smith LP, Surewicz WK (1997) The interaction between Alzheimer amyloid β(1–40) peptide and ganglioside GM1-containing membranes. FEBS Lett 402:95–98.

Choo-Smith LP, Garzon-Rodriguez W, Glabe CG, Surewicz WK (1997) Acceleration of amyloid fibril formation by specific binding of Aβ-(1–40) peptide to ganglioside-containing membrane vesicles. J Biol Chem 272:22987–22990.

Deleault NR, Lucassen RW, Supattapone S (2003) RNA molecules stimulate prion protein conversion. Nature 425:717–720.

Ding TT, Harper JD (1999) Analysis of amyloid-β assemblies using tapping mode atomic force microscopy under ambient conditions. In: Amyloid, prions, and other proteinaggregates (Wetzel R, ed), pp 510–525. New York: Academic.

Ehehalt R, Keller P, Haass C, Thiele C, Simons K (2003) Amyloidogenic processing of the Alzheimer β-amyloid precursor protein depends on lipid rafts. J Cell Biol 160:113–123.

Esler WP, Stimson ER, Jennings JM, Vinters HV, Ghilardi JR, Lee JP, Mantyh PW, Maggio JE (2000) Alzheimer's disease amyloid propagation by a template-dependent dock-lock mechanism. Biochemistry 39:6288–6295.

Harper JD, Lansbury Jr PT (1997) Models of amyloid seeding in Alzheimer's disease and scrapie: mechanistic truths and physiological consequences of the time-dependent solubility of amyloid proteins. Annu Rev Biochem 66:385–407.

Harper JD, Wong SS, Lieber CM, Lansbury Jr PT (1997a) Observation of metastable Aβ amyloid protofibrils by atomic force microscopy. Chem Biol 4:119–125.

Harper JD, Lieber CM, Lansbury Jr PT (1997b) Atomic force microscopic imaging of seeded fibril formation and fibril branching by the Alzheimer's disease amyloid-β protein. Chem Biol 4:951–959.

Harper JD, Wong SS, Lieber CM, Lansbury Jr PT (1999) Assembly of Aβ amyloid protofibrils: an in vitro model for a possible early event in Alzheimer's disease. Biochemistry 38:8972–8980.

Hayashi H, Igbavboa U, Hamanaka H, Kobayashi M, Fujita SC, Wood WG, Yanagisawa K (2002) Cholesterol is increased in the exofacial leaflet of synaptic plasma membranes of human apolipoprotein E4 knock-in mice. NeuroReport 13:383–386.

Hock C, Konietzko U, Papassotiropoulos A, Wollmer A, Streffer J, von Rotz RC, Davey G, Moritz E, Nitsch RM (2002) Generation of antibodies specific for β-amyloid by vaccination of patients with Alzheimer disease. Nat Med 8:1270–1275.

Igbavboa U, Avdulov NA, Schroeder F, Wood WG (1996) Increasing age alters transbilayer fluidity and cholesterol asymmetry in synaptic plasma membranes of mice. J Neurochem 66:1717–1725.

Kakio A, Nishimoto SI, Yanagisawa K, Kozutsumi Y, Matsuzaki K (2001) Cholesterol-dependent formation of GM1 ganglioside-bound amyloid β-protein, an endogenous seed for Alzheimer amyloid. J Biol Chem 276:24985–24990.

Kakio A, Nishimoto S, Yanagisawa K, Kozutsumi Y, Matsuzaki K (2002) Interactions of amyloid β-protein with various gangliosides in raft-like membranes: importance of GM1 ganglioside-bound form as an endogenous seed for Alzheimer amyloid. Biochemistry 41:7385–7390.

Kakio A, Nishimoto S, Kozutsumi Y, Matsuzaki K (2003) Formation of a membrane-active form of amyloid β-protein in raft-like model membranes. Biochem Biophys Res Commun 303:514–518.

Kayed R, Head E, Thompson JL, McIntire TM, Milton SC, Cotman CW, Glabe CG (2003) Common structure of soluble amyloid oligomers implies common mechanism of pathogenesis. Science 300:486–489.

Kim KS, Miler DL, Sapienza VJ, Chen C-MJ, Bai C, Grundke-Iqbal I, Currie JR, Wisniewski HM (1988) Production and characterization of monoclonal antibodies reactive to synthetic cerebrovascular amyoid peptide. Neurosci Res Commun 2:121–130.

Lee SJ, Liyanage U, Bickel PE, Xia W, Lansbury Jr PT, Kosik KS (1998) A detergent-insoluble membrane compartment contains A beta in vivo. Nat Med 4:730–734.

LeVine III H (1995) Soluble multimeric Alzheimer β (1–40) preamyloid complexes in dilute solution. Neurobiol Aging 16:755–764.

Lombardo JA, Stern EA, McLellan ME, Kajdasz ST, Hickey GA, Bacskai BJ, Hyman BT (2003) Amyloid-β antibody treatment leads to rapid normalization of plaque-induced neuritic alterations. J Neurosci 23:10879–10883.

Matsuzaki K, Horikiri C (1999) Interactions of amyloid β-peptide (1–40) with ganglioside-containing membranes. Biochemistry 38:4137–4142.

McLaurin J, Chakrabartty A (1996) Membrane disruption by Alzheimer β-amyloid peptides mediated through specific binding to either phospholipids or gangliosides. Implications for neurotoxicity. J Biol Chem 271:26482–26489.

McLaurin J, Franklin T, Fraser PE, Chakrabartty A (1998) Structural transitions associated with the interaction of Alzheimer beta-amyloid peptides with gangliosides. J Biol Chem 273:4506–4515.

McLaurin J, Cecal R, Kierstead ME, Tian X, Phinney AL, Manea M, French JE, Ambermon MH, Darabie AA, Brown ME, Janus C, Chishti MA, Horne P, Westaway D, Fraser PE, Mount HT, Przybylski M, St. George-Hyslop P (2002) Therapeutically effective antibodies against amyloid-beta peptide target amyloid-β residues 4–10 and inhibit cytotoxicity and fibrillogenesis. Nat Med 8:1263–1269.

Michikawa M, Yanagisawa K (1998) Apolipoprotein E4 induces neuronal cell death under conditions of suppressed de novo cholesterol synthesis. J Neurosci Res 54:58–67.

Morishima-Kawashima M, Ihara Y (1998) The presence of amyloid β-protein in the detergent-insoluble membrane compartment of human neuroblastoma cells. Biochemistry 37:15247–15253.

Naiki H, Gejyo F (1999) Kinetic analysis of amyloid fibril formation. Methods Enzymol 309:305–318.

Naiki H, Nakakuki K (1996) First-order kinetic model of Alzheimer's β-amyloid fibril extension in vitro. Lab Invest 74:374–383.

Naiki H, Hasegawa K, Yamaguchi I, Nakamura H, Gejyo F, Nakakuki K (1998) Apolipoprotein E and antioxidants have different mechanisms of inhibiting Alzheimer's β-amyloid fibril formation in vitro. Biochemistry 37:17882–17889.

Nakamura S, Nakayama H, Goto N, Ono F, Sakakibara I, Yoshikawa Y (1998) Histopathological studies of senile plaques and cerebral amyloidosis in cynomolgus monkeys. J Med Primatol 27:244–252.

Nichols MR, Moss MA, Reed DK, Lin W-L, Mukhopadhyay R, Hoh JH, Rosenberry TL (2002) Growth of β-amyloid (1–40) protofibrils by monomer elongation and lateral association. Characterization of distinct products by light scattering and atomic force microscopy. Biochemistry 41:6115–6127.

Parton RG (1994) Ultrastructural localization of gangliosides; GM1 is concentrated in caveolae. J Histochem Cytochem 42:155–166.

Roher AE, Lowenson JD, Clarke S, Wolkow C, Wang R, Cotter RJ, Reardon IM, Zurcher-Neely HA, Heinrikson RL, Ball MJ, Greenberg BD (1993) Structural alterations in the peptide backbone of beta-amyloid core protein may account for its deposition and stability in Alzheimer's disease. J Biol Chem 268:3072–3083.

Sawamura N, Morishima-Kawashima M, Waki H, Kobayashi K, Kuramochi T, Frosch MP, Ding K, Ito M, Kim TW, Tanzi RE, Oyama F, Tabira T, Ando S, Ihara Y (2000) Mutant presenilin 2 transgenic mice. A large increase in the levels of Aβ42 is presumably associated with the low density membrane domain that contains decreased levels of blycerophospholipids and sphingomyelin. J Biol Chem 275:27901–27908.

Selkoe DJ (1997) Alzheimer's disease: genotypes, phenotypes, and treatments. Science 275:630–631.

Shapira R, Austin GE, Mirra SS (1988) Neuritic plaque amyloid in Alzheimer's disease is highly racemized. J Neurochem 50:69–74.

Simons K, Ikonen E (1997) Functional rafts in cell membranes. Nature 387:569–572.

Smit JW, Meijer CJ, Decary F, Feltkamp-Vroom TM (1974) Paraformaldehyde fixation in immunofluorescence and immunoelectron microscopy. Preservation of tissue and cell surface membrane antigens. J Immunol Methods 6:93–98.

Solomon B, Koppel R, Frankel D, Hanan-Aharon E (1997) Disaggregation of Alzheimer β-amyloid by site-directed mAb. Proc Natl Acad Sci USA 94:4109–4112.

Suzuki N, Iwatsubo T, Odaka A, Ishibashi Y, Kitada C, Ihara Y (1994) High tissue content of soluble β 1–40 is linked to cerebral amyloid angiopathy. Am J Pathol 145:452–460.

Telling GC, Scott M, Mastrianni J, Gabizon R, Torchia M, Cohen FE, DeArmond SJ, Prusiner SB (1995) Prion propagation in mice expressing human and chimeric PrP transgenes implicates the interaction of cellular PrP with another protein. Cell 83:79–90.

Yanagisawa K, Ihara Y (1998) GM1 ganglioside-bound amyloid β-protein in Alzheimer's disease brain. Neurobiol Aging 19:S65–S67.

Yanagisawa K, Odaka A, Suzuki N, Ihara Y (1995) GM1 ganglioside-bound amyloid β-protein (Aβ): a possible form of preamyloid in Alzheimer's disease. Nat Med 1:1062–1066.

Yanagisawa K, McLaurin J, Michikawa M, Chakrabartty A, Ihara Y (1997) Amyloid β-protein (Aβ) associated with lipid molecules: immunoreactivity distinct from that of soluble Aβ. FEBS Lett 420:43–46.

THE JOURNAL OF BIOLOGICAL CHEMISTRY
Vol. 279, No. 12, Issue of March 19, pp. 11984–11991, 2004
Printed in U.S.A.

Modulation of Amyloid Precursor Protein Cleavage by Cellular Sphingolipids*

Received for publication, September 4, 2003, and in revised form, January 8, 2004
Published, JBC Papers in Press, January 10, 2004, DOI 10.1074/jbc.M309832200

Naoya Sawamura‡§, Mihee Ko‡, Wenxin Yu‡, Kun Zou‡, Kentaro Hanada¶, Toshiharu Suzuki‖, Jian-Sheng Gong‡, Katsuhiko Yanagisawa‡, and Makoto Michikawa‡ ‡‡**

*From the ‡Department of Dementia Research, National Institute for Longevity Sciences, 36-3 Gengo, Morioka, Obu, Aichi 474-8522, Japan, the §Japan Society for the Promotion of Science, Tokyo 102-8471, Japan, the ¶Department of Biochemistry and Cell Biology, National Institute of Infectious Diseases, 1-23-1, Toyama, Shinjuku-ku, Tokyo 162-8640, Japan, the ‖Laboratory of Neuroscience, Graduate School of Pharmaceutical Sciences, Hokkaido University, Sapporo 060-0812, Japan, and the **Organization of Pharmaceutical Safety and Research of Japan, Tokyo 100-0013, Japan*

Lipid rafts and their component, cholesterol, modulate the processing of β-amyloid precursor protein (APP). However, the role of sphingolipids, another major component of lipid rafts, in APP processing remains undetermined. Here we report the effect of sphingolipid deficiency on APP processing in Chinese hamster ovary cells treated with a specific inhibitor of serine palmitoyltransferase, which catalyzes the first step of sphingolipid biosynthesis, and in a mutant LY-B strain defective in the LCB1 subunit of serine palmitoyltransferase. We found that in sphingolipid-deficient cells, the secretion of soluble APPα (sAPPα) and the generation of C-terminal fragment cleaved at α-site dramatically increased, whereas β-cleavage activity remained unchanged, and the ε-cleavage activity decreased without alteration of the total APP level. The secretion of amyloid β-protein 42 increased in sphingolipid-deficient cells, whereas that of amyloid β-protein 40 did not. All of these alterations were restored in sphingolipid-deficient cells by adding exogenous sphingosine and in LY-B cells by transfection with *cLCB1*. Sphingolipid deficiency increased MAPK/ERK activity and a specific inhibitor of MAPK kinase, PD98059, restored sAPPα level, indicating that sphingolipid deficiency enhances sAPPα secretion via activation of MAPK/ERK pathway. These results suggest that not only the cellular level of cholesterol but also that of sphingolipids may be involved in the pathological process of Alzheimer's disease by modulating APP cleavage.

The amyloid β-peptide (Aβ)[1] is the principle constituent of senile plaques found in Alzheimer's disease (AD) brains and is generated by proteolysis of an integral membrane protein, the amyloid precursor protein (APP). APP is metabolized via at least two post-translational pathways, one of which is a nonamyloidogenic pathway mediated by α-secretase proteolytically producing soluble APP (sAPPα), the dominant processing product; this cleavage generates the residual 10-kDa CTF (CTFα). Previous studies have shown that the activation of signal transduction pathways including protein kinase C (PKC) (1–3), mitogen-associated protein kinase (MAPK) (4), and growth factors (5) alter the relative amounts of sAPPα and Aβ production. The other cleavage is mediated by β-secretase, generating several proteolytic C-terminal fragments (CTFs), namely, CTFβ and CTFε, and γ-secretase, producing either a 40-residue protein (Aβ40) or a 42-residue protein (Aβ42) from CTFβ. The cleavages at residues 40–42 are referred to as γ-cleavage, and the cleavage at residues 49–52 are referred to as ε-cleavage (6).

Recent studies revealed that the prevalence of AD is linked to the serum cholesterol level and that sAPPα secretion and Aβ generation are modulated by the cellular cholesterol level (7–13). It is also suggested that APP processing and Aβ generation are associated with membrane microdomains, known as lipid rafts, that are rich in cholesterol and sphingolipids and are also the principal compartment in which Aβ is found (13–18).

The cholesterol content in lipid rafts has been shown to contribute to the integrity of the raft structure and the functions of the rafts in signaling and membrane trafficking (19–21). In addition, several studies showed that sphingolipids modulate raft functions; the reduction in the cellular sphingolipid level renders glycosyl phosphatidylinositol (GPI)-anchored proteins more sensitive to phosphatidylinositol-specific phospholipase C (22) and also enhances the solubility of GPI-anchored proteins in Triton X-100 (23). The blockade of ceramide synthesis was shown to inhibit folate uptake via GPI-anchored receptors (24) and to enhance the conversion of the prion protein to its scrapie form (25–27). These studies indicate that the cellular levels of cholesterol and sphingolipids modulate the functions of lipid rafts. Therefore, the evidence that the cholesterol level in lipid rafts can modulate APP processing reasonably raises the question of whether cellular sphingolipids also modulate APP processing and Aβ generation. However, the participation of sphingolipids in APP processing remains undetermined.

To address this issue, we examined the alterations in APP processing and Aβ generation in sphingolipid-deficient cells using ISP-1 (myriocin), a potent inhibitor of serine palmitoyltransferase (SPT) (28), and a CHO-K1-cell-derived mutant cell line, the LY-B strain, which has a defect in the LCB1 subunit of SPT and is therefore incapable of *de novo* synthesis of any sphingolipid species (29). Our findings indicate that not only

* This work was supported by Research Grant for Longevity Sciences and Brain Science Research H14-Cyoju-010 from the Ministry of Health and Welfare, Japan, and by funds from the Program for Promotion of Fundamental Studies in Health Sciences of the Organization for Pharmaceutical Safety and Research of Japan. The costs of publication of this article were defrayed in part by the payment of page charges. This article must therefore be hereby marked "*advertisement*" in accordance with 18 U.S.C. Section 1734 solely to indicate this fact.

‡‡ To whom correspondence should be addressed. Tel.: 81-562-46-2311; Fax: 81-562-44-6594; E-mail: michi@nils.go.jp.

[1] The abbreviations used are: Aβ, amyloid β-protein; AD, Alzheimer's disease; CHO, Chinese hamster ovary; FBS, fetal bovine serum; SPT, serine palmitoyltransferase; GPI, glycosylphosphatidylinositol; APP, amyloid precursor protein; CTF, C-terminal fragment; ELISA, enzyme-linked immunosorbent assay; MAPK, mitogen-associated protein kinase; ERK, extracellular signal-regulated kinase; PKC, protein kinase C.

the cellular cholesterol level but also the sphingolipid level modulates APP processing.

MATERIALS AND METHODS

Antibodies—The monoclonal antibody 22C11, which recognizes amino acids 66–81 of the N terminus of APP, was purchased from Chemicon International (Temecura, CA). The monoclonal antibodies used were BA27, which is specific for the Aβ1–40 terminal site; BC05, which is specific for the Aβ42 terminal site; and BNT77, which was raised against Aβ11–28 but recognizes Aβ11–16; all of these antibodies have been characterized previously (30). The monoclonal antibody 6E10 (raised against Aβ1–17) was purchased from Senetek PLC (Maryland, MO). The rabbit polyclonal antibody, UT-18 (raised against APP695-(676–695)) was used to detect cellular APP and its C-terminal fragments (31). The rabbit polyclonal antibody, G530, which was raised against rat Aβ1–16, was used to detect rodent sAPPα (32). The rabbit polyclonal antibodies that recognize phospho-independent PKCα, PKCδ, PKCε, and PKCγ were purchased from Santa Cruz Biotechnology, Inc. (Santa Cruz, CA).

Cell Culture—The CHO-K1 cell-derived mutant cell line, the LY-B strain, has been previously established (29). LY-B/cLCB1, a corrected revertant of the LY-B strain, was previously obtained by the stable transfection of LY-B cells with the cDNA encoding the hamster LCB1 subunit of SPT (29). Ham's F-12 medium supplemented with 10% fetal bovine serum was used as the normal culture medium. CHO-K1 cells stably expressing APP751 (APP-CHO-K1) were used for determining APP processing and Aβ generation. To deplete sphingolipids, APP-CHO-K1 cells were treated with 1 μM myriosin (ISP-1; purchased from BIOMOL Research Laboratories). The Nutridoma-BO medium (Ham's F-12 medium containing 1% Nutridoma-SP (Roche Applied Science), 0.1% fetal bovine serum (FBS), and 10 μM sodium oleate-bovine serum albumin complex) was used as the sphingolipid-deficient medium. For cultivation in sphingolipid-deficient medium, the cells were seeded, incubated in the normal culture medium at 37 °C for 1 day, and, after washing twice with serum-free Ham's F-12 medium, were cultured in the Nutridoma-BO medium for 2 days. In the experiment on the pharmacological inhibition of SPT in APP-CHO-K1 cells, the Nutridoma-BO medium was supplemented with 1 μM ISP-1, and the levels of sphingolipids were recovered with concurrent treatment with 1 μM D-erythro-sphingosine (Matreya, Inc., Pleasant Gap, PA) as described previously (28).

ELISA—Two-site ELISA for Aβ40 and Aβ42 was carried out as previously described (30, 33). BNT77 was coated as the capture antibody, whereas BA27 (for Aβ40) and BC05 (for Aβ42) were used as the detection antibodies following conjugation with horseradish peroxidase.

Protein Preparation—Cultured cells grown in 10-cm^2 dishes were washed twice with ice-cold phosphate-buffered saline and then collected by scraper. The cells were then centrifuged at 1,000 × *g* for 10 min, and the cell pellet was homogenized in Tris saline (50 mM Tris-HCl, pH 7.4, 150 mM NaCl), containing 1% Triton X-100 and protease inhibitors (Complete), followed by homogenization using a motor-driven Teflon homogenizer. The homogenates were then centrifuged at 200,000 × *g* for 20 min at 4 °C in a TLX ultracentrifuge (Beckman). The supernatants were collected for biochemical analyses. Protein concentrations were determined using the bicinchoninic acid protein assay kit (Pierce). Aliquots of the supernatant samples containing equal amounts of protein were subjected to 7.5% or 4–20% SDS-PAGE for immunoblot analysis as described previously (34).

Lipid Analysis—The metabolic labeling of lipids with [^{14}C]serine in APP-CHO-K1 cells in the presence or absence of 1 μM of ISP-1 was performed as described previously (35). The rate of lipid labeling was corrected for each protein concentration.

Immunoblot Analysis—The proteins separated using SDS-PAGE were electrophoretically transferred onto a polyvinylidene difluoride membrane (Millipore, Bedford, MA). Nonspecific binding was blocked with 5% fat-free milk in phosphate-buffered saline containing 0.1% Tween 20. The blots were then incubated with primary antibodies overnight at 4 °C. For the detection of both primary monoclonal and polyclonal antibodies, appropriate peroxidase-conjugated secondary antibodies were used in conjunction with SuperSignal Chemiluminesence (Pierce) to obtain images that were saved on film. The primary antibodies used were as follows: monoclonal antibodies; 22C11, at a final concentration of 5 μg/ml; 6E10, at a final concentration of 5 μg/ml; polyclonal antibodies, G530, which recognizes rodent sAPPα, diluted at 1:1,000; and UT-18, which recognizes the C terminus of APP, diluted at 1: 500. The membrane fractions were prepared and subjected to immunoblot analysis using anti-PKCα, PKCδ, PKCε, and PKCγ antibodies diluted at 1:1000.

Preparation of Membrane Fractions—APP C-terminal fragment generation was performed in cell-free systems as described previously (36). CHO-K1 cells were suspended in Buffer H (20 mM HEPES, 150 mM NaCl, 10% glycerol, 5 mM EDTA, pH 7.4) containing protease inhibitors (Complete), and thereafter the postnuclear supernatant was collected. The microsomal membrane was precipitated from the postnuclear supernatant by centrifugation at 100,000 × *g* for 1 h at 4 °C and resuspended in Buffer H containing protease inhibitors and incubated 37 °C for 2 h to generate CTFε. The aliquots of the samples kept on ice for 2 h were used as negative controls. At the end of the assay, the microsomal membrane samples were separated into pellet and supernatant fractions by ultracentrifugation at 100,000 × *g* for 1 h at 4 °C. Each pellet fraction was suspended in SDS sample buffer, and each supernatant fraction was diluted with an equal volume of 2× SDS sample buffer to be used for immunoblot analysis.

PKC Translocation Assay—The PKC translocation assay was carried out as described previously (37). APP-CHO-K1 cells were incubated for 2 days in the Nutridoma-BO medium in the absence or presence of 1 μM ISP-1 or 1 μM ISP-1 plus 1 μM sphingosine for 48 and 73 h as indicated. Wild-type CHO, LY-B, and LY-B/cLCB1 cells were also incubated in Nutridoma-BO medium for 48 h. Thereafter, the cells were washed and scraped into 200 μl of homogenization buffer (20 mM Tris-HCl, pH 7.4, 1 mM EDTA, 1 mM EGTA, protease inhibitors (Complete)), lysed by homogenizer, and centrifuged at 100,000 × *g* for 1 h at 4 °C. The pellets were resonicated in 200 μl of homogenization buffer supplemented with 1% Triton X-100 and centrifuged at 100,000 × *g* for 1 h at 4 °C, yielding solubilized particulate fractions. The protein concentration was determined, and the fractions were analyzed by immunoblotting using antibodies, which recognize phosphorus-independent PKCα, PKCδ, PKCε, and PKCγ.

Purification of the Lipid Raft Fraction—The lipid raft fraction was obtained from each cell line according to an established method previously reported (33, 38). One milliliter of each fraction was sequentially collected from the top of the gradient. The extraction of lipids and subsequent determination of the amount of cholesterol and phospholipids in each sample were carried out according to previously described methods (39).

Statistical Analysis—Statistical analysis was carried out using StatView computer software (Macintosh, version 5.0; Abacus Concepts Inc., Berkeley, CA). A p value < 0.05 was considered to indicate statistical significance.

RESULTS

Sphingolipid Deficiency Induced by SPT Enhanced sAPPα Secretion in CHO-K1 Cell Lines—We used CHO-K1 cells stably transfected with human APP751 cDNA (APP-CHO-K1) (40) and treated these cells with myriosin (designated as ISP-1), which is a potent inhibitor of SPT. Using this inhibitor, we obtained the pharmacological cell model of sphingolipid deficiency (28). We determined the level of sphingolipid synthesis in APP-CHO-K1 cells treated with ISP-1 in a sphingolipid-deficient medium. Fig. 1*a* shows that the rate of *de novo* sphingomyelin synthesis in ISP-1-treated APP-CHO-K1 cells decreased significantly as previously reported (28, 29). Using this culture system, we determined APP levels secreted from ISP-1-treated and nontreated APP-CHO-K1 cells and cellular APP levels in these cells. Immunoblot analysis using the 6E10 antibody, which recognizes the C terminus of human sAPPα, showed that the secreted sAPPα level in sphingolipid-deficient cells is significantly higher (about 3.1-fold) than that in nontreated cells (Fig. 1, *b* and *c*). These results indicate that α-cleavage is activated in CHO-K1 cells treated with ISP-1. The immunoblot analysis of cellular APP using the 22C11 antibody, which recognizes the N terminus of APP, and the UT-18 antibody, which recognizes the C terminus of APP, showed that treatment with ISP-1 does not seem to affect cellular total APP level but significantly reduces the levels of the mature forms (*N*- and *O*-glycosylated forms) of APP (Fig. 1, *b* and *c*). Treatment with ISP-1 does not affect the cellular α-tubulin level.

Effect of Sphingolipid Deficiency on Generation of CTFα, CTFβ, and CTFε in CHO-K1 Cell Lines—Next, we determined

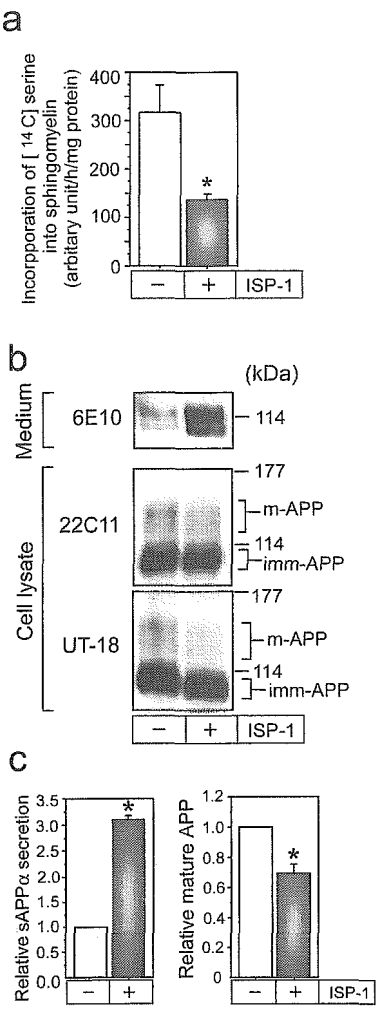

FIG. 1. **Sphingolipid deficiency reduces the levels of sAPPαreleased from APP-CHO-K1 cells.** APP-CHO-K1 cells were seeded in the 10% FBS containing medium in 10-cm^2 culture dishes. Twenty-four hours after plating, the cells were washed twice with Ham's F-12, refed with sphingolipid-deficient medium (Nutridoma-BO medium) in the presence or absence of 1 μM ISP-1, and maintained for another 2 days. *a*, using these cells, sphingomyelin incorporation rate was determined as described under "Materials and Methods." *b*, for the determination of the levels of released sAPPα and cellular APP in cultured cells with or without treatment, the cultured media were collected, and the cells were harvested. The levels of secreted sAPPα in the medium and intracellular APP were determined by immunoblot analysis using 6E10 (for sAPPα) and 22C11 and UT-18 (for intracellular APP). *c*, the immunoreactivities of each sample to the 6E10 antibody in the medium and to the UT-18 antibody in the cell lysate were quantified using a Macintosh computer with software (National Institutes of Health Image) for densitometric analysis. The data represent the means ± S.E. for triplicate experiments. *, $p < 0.005$ *versus* ISP-1 (−). Three independent experiments showed similar results.

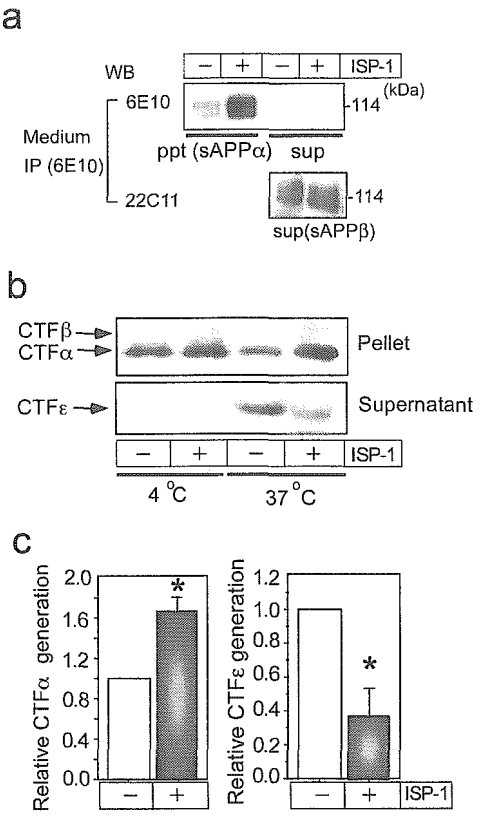

FIG. 2. **Effect of sphingolipid deficiency on secretion of sAPPβand generation of CTFs in APP-CHO-K1 cells treated with ISP-1.** APP-CHO-K1 cells were seeded in the 10% FBS-containing medium in 10-cm^2 culture dishes. Twenty-four hours after plating, the cells were refed with the Nutridoma-BO medium, treated with or without 1 μM ISP-1, and maintained for another 48 h. *a*, the culture media were harvested to detect sAPPα and sAPPβ as described under "Materials and Methods." sAPPα in each culture medium was immunoprecipitated with the 6E10 antibody. The resultant supernatant was analyzed to detect sAPPβ by immunoblot analysis using the 22C11 antibody. *b*, the pellet and supernatant fractions from microsomal membrane were obtained by further ultracentrifugation as described under "Materials and Methods." The generation of CTFα and CTFβ were detected by immunoblot analysis with the UT18 antibody at ~10 kDa in the pellet fraction sample, and the generation of CTFε was detected with the UT18 antibody at ~6 kDa in the samples of the supernatant fraction after 2 h of incubation. *c*, the intensities of the bands for CTFα at 4 °C (*left panel*) and CTFε at 37 °C (*right panel*) after 2 h incubation were determined using a Macintosh computer with software (National Institutes of Health Image) for densitometric analysis. The data represent the mean ± S.E. for triplicate experiments. *, $p < 0.05$ *versus* ISP-1 (−). Three independent experiments showed similar results. *WB*, Western blot; *sup*, supernatant; *ppt*, pellet.

the sAPPβ levels in the conditioned media of the SPT-treated and nontreated APP-CHO-K1 cells. We first immunoprecipitated sAPPα in the conditioned media of APP-CHO-K1 cells using the 6E10 antibody, and the remaining supernatant was used for sAPPβ detection. The immunoblot analysis of the remaining supernatant using the 22C11 antibody showed that ISP-1 treatment does not have any significant effect on sAPPβ levels (Fig. 2*a*). We next examined whether the level of C-terminal fragments of APP differ between ISP-1-treated and nontreated APP-CHO-K1 cells. We prepared microsomal fractions from each cell line and incubated them at 0 or 37 °C for 2 h. In APP-CHO-K1 cells, CTFα was mainly detected at 10 kDa, and CTFβ was weakly detected (Fig. 2*b*). When the cells were treated with ISP-1, the intensity of the band representing CTFα increased significantly at 4 °C (Fig. 2, *b* and *c*). Compatible with the data shown in Figs. 1*b* and 2*a*, these findings indicate that α-cleavage is activated in CHO-K1 cells treated with the SPT inhibitor. It was reported that the incubation of the microsomal fraction generates CTFε detected at ~6.5 kDa, which migrates below the major APP C-terminal fragments arising from CTFα and CTFβ (6, 36, 41). We also observed that CTFε was generated in the microsomal membranes of APP-CHO-K1 cells after a 2-h incubation (Fig. 2*b*). The level of CTFε generated in the membrane fraction of the ISP-1-treated APP-CHO-K1 cells decreased significantly compared with that of the nontreated cells (Fig. 2*b*), and the level of CTFε in the ISP-1-treated cells decreased to 40% of that of the nontreated cells (Fig. 2*c*). These results indicate that the extent of ε-cleavage decreases in CHO-K1 cells treated with the SPT inhibitor.

Altered Processing of APP Was Restored by Adding Exogenous Sphingosine in ISP-1-treated Cells—To determine that

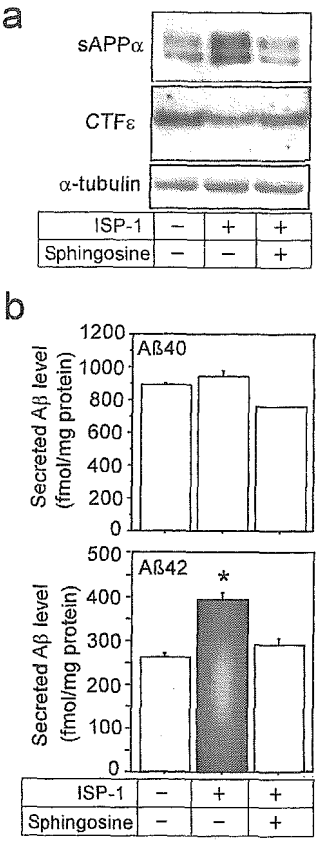

FIG. 3. **Cellular sphingolipid level modulated sAPPαsecretion, the cellular CTFεlevel, and the secretion of Aβ40 and Aβ42 in APP-CHO-K1 cells.** Twenty-four hours after plating in the 10% FBS-containing medium in 10-cm^2 culture dishes, the culture medium was changed with the sphingolipid-deficient medium with no ISP-1, 1 μM ISP-1, or 1 μM ISP-1 plus 1 μM D-erythro-sphingosine. The cultures were then maintained for another 48 h, followed by washing with phosphate-buffered saline twice, and the culture medium was harvested, and the microsomal fractions were prepared as described above. *a*, sAPPα in the cultured medium was detected by immunoblot analysis with the 6E10 antibody, and CTFε generated in the membrane pellet after incubation at 37 °C for 2 h was detected with the UT18 antibody. Three independent experiments showed similar results. *b*, the levels of Aβ40 and Aβ42 were quantified by sandwich ELISA using the BNT77 and BC05 antibodies. The data represent the means ± S.E. for triplicate experiments. *, $p < 0.05$ *versus* ISP-1 (−)/sphingosine (−) and ISP-1 (+)/sphingosine (+).

the increased sAPPα level is due to sphingolipid deficiency, we examined whether the addition of exogenous sphingosine restores the altered APP level in ISP-1-treated CHO-K1 cells. As shown in Fig. 3*a*, when exogenous sphingosine was concurrently treated with ISP-1, the sAPPα level decreased to that of the nontreated cells. Similarly, the CTFε level decreased in the ISP-1-treated cells, which was also restored by adding exogenous sphingosine (Fig. 3*a*). There was no difference in the cellular α-tubulin level between these cultures. We further determined the levels of Aβ40 and Aβ42 in the nontreated and ISP-1-treated cultures by two-site ELISA. ISP-1 treatment increased Aβ42 level (about 1.6-fold that of the nontreated cells), whereas it had no effect on the Aβ40 level (Fig. 3*b*). When exogenous sphingosine was concurrently treated with ISP-1, the Aβ42 level in the culture medium was restored to that of the nontreated cells (Fig. 3*b*).

MAPK/ERK, but Not PKC Activity Is Involved in the Enhancement of sAPPα Secretion Caused by Sphingolipid Deficiency—It has been demonstrated that sAPPα secretion is regulated in either a PKC-dependent or -independent manner that involves the activation of tyrosine kinases (1, 2, 42). Moreover, the MAPK signaling pathway has recently been implicated in both PKC and tyrosine kinase receptor regulations of APP processing (4, 43). We therefore assessed which, if any, of these kinases mediates the effect of sphingolipid deficiency on sAPPα secretion. We found that the ERK activity and the sAPPα secretion level increased in the APP-CHO cells treated with ISP-1 without a change in the level of total ERK, and these increases were restored by concurrent treatment with PD98059, a specific inhibitor of MAPK/ERK kinase (Fig. 4*a*). We also examined the levels of PKC that translocated into the plasma membrane in sphingolipid-deficient cells and noted that the levels of PKCα, PKCδ, PKCε, and PKCγ translocated into the plasma membrane fraction are not altered in sphingolipid-deficient cells (Fig. 4*b*). Furthermore, we carried out experiments to confirm whether sphingolipid deficiency also modulates the processing of endogenous APP in wild-type CHO cells. As shown in Fig. 4*c*, the sAPPα secretion level and ERK activity increased when sphingolipid level decreased following ISP-1 treatment, without a change in the level of total ERK; these increases were restored by concurrent treatment with PD98059, a specific inhibitor of MAPK/ERK kinase, and sphingosine

sAPPα Secretion Level Also Increased in CHO-K1 Cell Mutant Strain (LY-B) Defective in the LCB1 Subunit of SPT—To confirm whether sphingolipid deficiency induced by ISP-1 treatment is a sphingolipid-specific phenomenon, we further examined the effect of sphingolipid deficiency on APP processing using the CHO-K1 cell mutant strain, LY-B, defective in the LCB1 subunit of SPT, which is unable to synthesize any sphingolipid species *de novo* (29). Another mutant CHO-K1 cell line, the LY-B/cLCB1 strain, which is the complemented transformant of LY-B, was also used (29). Because these cell lines express only endogenous hamster APP, we used G530 antibody, which recognizes rodent APP. When these cells were cultured in a sphingolipid-deficient medium for 2 days, the sphingomyelin level in LY-B cells decreased to ~15% of that in wild-type CHO-K1 cells (44). The sAPPα secretion level significantly increased in LY-B cells, whereas the total APP level and the level of α-tubulin, an internal control, remained unchanged; however, such an increase was not noted in LY-B/cLCB1 cells (Fig. 5*a*). We further examined the effect of PD98059 on the secreted sAPPα level to determine whether the increase in the sAPPα level is mediated by MAPK/ERK activity. Similarly to the case of ISP-1-treated cells shown in Fig. 4, both ERK activity and the sAPPα secretion level increased in the sphingolipid-deficient cells, LY-B cells, whereas total ERK levels and the level of α-tubulin, an internal control, remained unchanged (Fig. 5*b*). These increases in ERK activity and the sAPPα level were restored by transfection with c*LCB1* or treatment with PD98059 or sphingosine (Fig. 5*b*). These results indicate that sphingolipid deficiency increases sAPPα secretion level via ERK activation. In contrast, the levels of PKCα, PKCδ, PKCε, and PKCγ that translocated into the plasma membrane fraction were not altered in these three cell lines (Fig. 5*c*).

Characterization of Lipid Rafts of Wild-type CHO, LY-B, and LY-B/cLCB1 Cells and APP Localization in the Lipid Rafts in These Cell Lines—We finally examined the effect of sphingolipid deficiency on lipid composition in lipid raft fractions and APP localization in lipid rafts. We treated cell lysate of CHO, LY-B, and LY-B/cLCB1 cells with Triton X-100, separated them in a sucrose density gradient (33, 38), and determined the levels of cholesterol, phospholipids, and GM1, a marker for lipid rafts, in each fraction. As shown in Fig. 6*a*, the raft fraction (fraction 4) enriched in GM1 contained 20 and 18% of total phospholipids in the wild-type CHO and LY-B/cLCB1 cells, respectively, whereas 12% of total phospholipids was recovered in fraction 4 of the LY-B cells. In contrast, the dis-

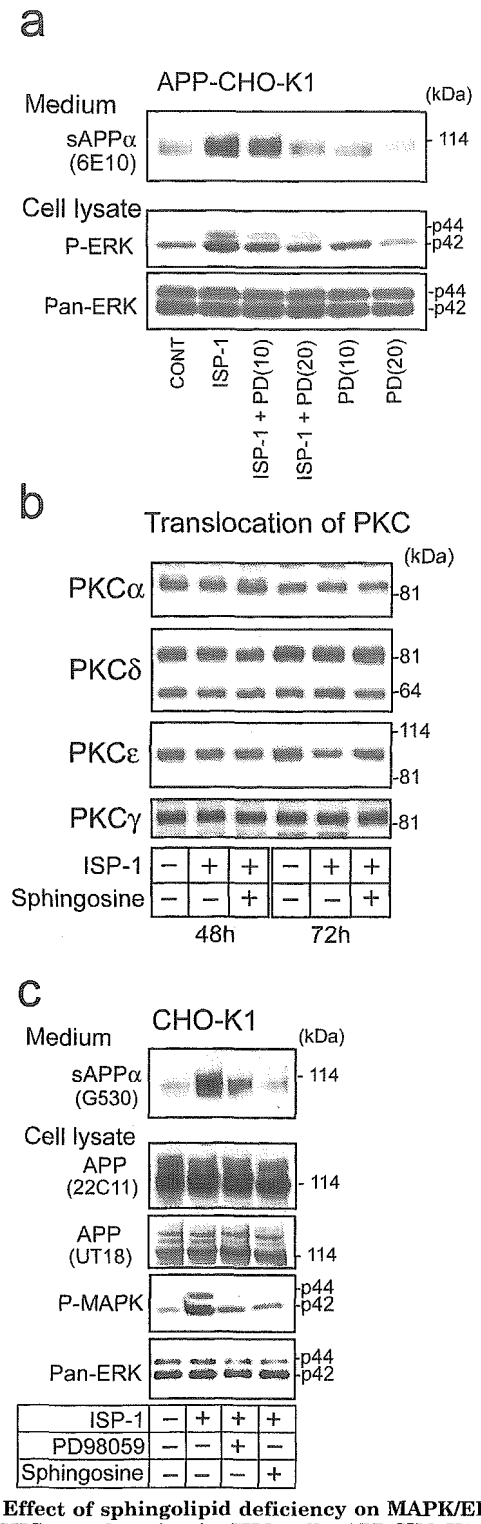

FIG. 4. **Effect of sphingolipid deficiency on MAPK/ERK activity and PKC translocation in CHO cells.** APP-CHO-K1 cells were seeded in the 10% FBS-containing medium in 10-cm^2 culture dishes. Twenty-four hours after plating, the cells were refed with the Nutridoma-BO medium and treated with or without 1 μM ISP-1 or other reagent and maintained for another 48 h. Thirty minutes before changing the medium, PD98059 was added to the cultures, and then the medium was changed to a fresh Nutridoma-BO medium containing the indicated reagent(s). *a*, four hours after the medium change, the culture medium and the cells were harvested to detect sAPPα, phospho-ERK, and total ERK as described under "Materials and Methods." *b*, the membrane fractions were prepared and subjected to immunoblot analysis using anti-PKCα, PKCδ, PKCε, and PKCγ antibodies as described under "Materials and Methods." *c*, six hours after the medium change, the culture medium and the cells were harvested to detect sAPPα, phospho-ERK, and total ERK as described under "Materials and Methods."

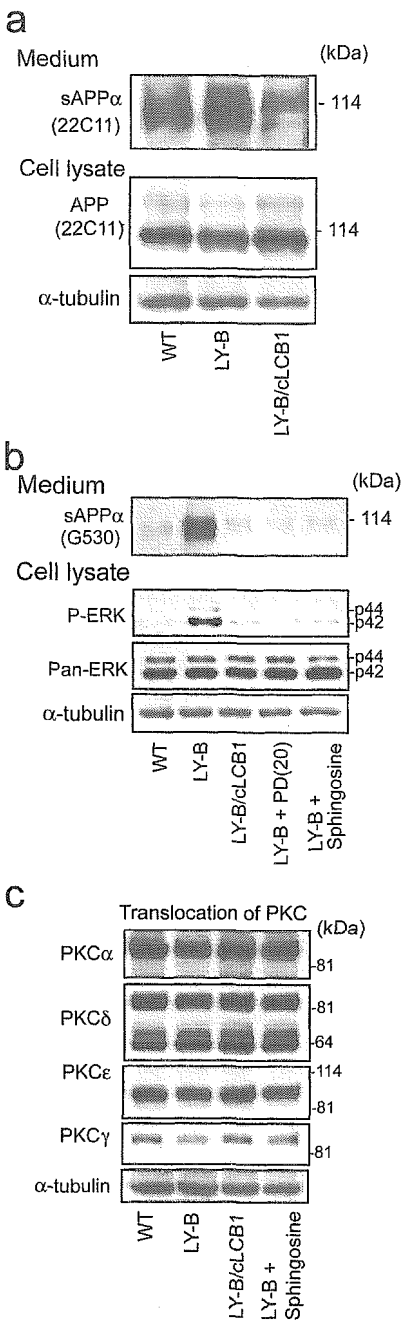

FIG. 5. **Effect of MAPK/ERK activity on the levels of APP secreted from wild-type CHO, LY-B, and LY-B/cLCB1 cells.** Wild-type CHO (*WT*), LY-B, and LY-B/cLCB1 cells were seeded in the 10% FBS containing medium in 10-cm^2 culture dishes. Twenty-four hours after plating, the cells were refed with the Nutridoma-BO medium and maintained for another 48 h. *a*, the culture medium was again changed to a fresh Nutridoma-BO medium. The cultures were then further incubated for 6 h, and the culture media and the cells were harvested to detect sAPPα and cellular APP using 22C11 antibody. *b*, for determination of the effect of ERK activity on sAPPα secretion, PD98059 was pretreated 30 min before changing to a fresh Nutridoma-BO medium containing the indicated reagent(s). Six hours following the medium change, the culture medium and the cells were harvested to detect sAPPα, phospho-ERK, and total ERK as described under "Materials and Methods." *c*, the membrane fractions were prepared and subjected to immunoblot analysis using anti-PKCα, PKCδ, PKCε, and PKCγ antibodies as described under "Materials and Methods."

tribution peak of cholesterol in the raft fraction in LY-B cells remained similar or rather higher levels compared with those for the other two genotypes (Fig. 6*a*). These results suggest that the structure of the raft domain may have been altered, and thus their function deteriorated. We further determined the

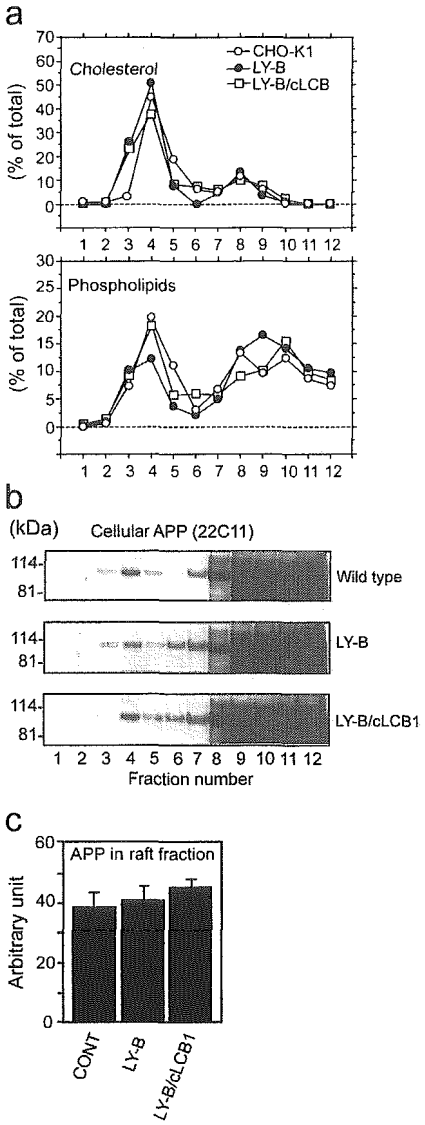

FIG. 6. **The levels of cholesterol, sphingolipids, and APP recovered in lipid rafts of wild-type, LY-B, and LY-B/cLCB1 cells.** Wild-type CHO (*WT*), LY-B, and LY-B/cLCB1 cells were seeded in the 10% FBS containing medium in 10-cm^2 culture dishes. Twenty-four hours after plating, the culture medium was changed with the Nutridoma-BO medium, and the cells were maintained for another 48 h. The cells were then harvested, homogenized in the presence of 1% Triton X-100, and fractionated by sucrose density gradient centrifugation as described previously (33, 38). The fractions were collected from the top gradient, and 12 fractions were obtained. *a*, the levels of cholesterol and phospholipids in each fraction were determined as described previously (39). *b*, for immunoblot analysis using the 22C11 antibody, the cells were harvested, homogenized, and subjected to immunoblot analysis as described under "Materials and Methods." *c*, the intensity of APP signal in the lipid rafts fraction (fraction 4) of each cell line was analyzed. The data are the means ± S.E. for triplicate experiments. There is no significant difference between these three lines. *a–c*, three independent experiments showed similar results.

APP levels in these fractions by immunoblot analysis using the monoclonal antibody, 22C11, and the intensities of APP signal in the raft fraction were quantified by densitometric analysis. As shown in Fig. 6 (*b* and *c*), the amount of APP recovered in the raft fraction of each cell line was at a similar level.

DISCUSSION

In this study, we found that the sphingolipid deficiency induced by the SPT inhibitor enhances α-cleavage of APP without altering the total amount of cellular APP. These alterations are restored by adding exogenous sphingosine. The enhanced α-cleavage of APP caused by sphingolipid deficiency is confirmed in cells whose sphingolipid synthesis is genetically defective, indicating that cellular sphingolipid level is a critical modulator of APP processing to secrete sAPPα. We also found that MAPK/ERK is activated in sphingolipid-deficient cells and that the inhibition of MAPK/ERK pathway restores sAPPα level, suggesting that sphingolipid deficiency enhances sAPPα secretion via activation of the MAPK/ERK pathway.

It was shown that APP cleavage by α-secretase is dependent on the cellular cholesterol level (12), and sAPPα secretion and Aβ42 generation are determined by the dynamic interactions of APP with lipid rafts (15, 16, 18), probably because of the alteration of both APP and β-secretase partitioning into lipid rafts (13, 17). Because cholesterol depletion is postulated to disrupt raft functions (45), our present results suggest that the depletion of sphingolipids, another major component of lipid rafts, affects lipid raft functions, thereby altering APP processing as noted in cholesterol-depleted cells.

A question arises of how sphingolipid deficiency alters APP processing to enhance sAPPα secretion. Because PKC and ERK modulate sAPPα secretion (1–4, 43, 46), we examined whether PKC and ERK are responsible for the increased levels of sAPPα secreted from sphingolipid-deficient cells. We found that the decreased sphingolipid level in sphingolipid-deficient cells enhances ERK activity (Figs. 4 and 5) and that the inhibition of ERK activity by PD98059 restores the increase in sAPPα level in sphingolipid-deficient cultures, suggesting that increased levels of ERK activity associated with sphingolipid deficiency enhance sAPPα secretion. In contrast, we did not observe any alteration in the amount of PKC that translocated to the plasma membrane in the sphingolipid-deficient cells. Although ERK is located in the downstream of the PKC signaling cascade (4, 43, 46, 47), these results suggest that sphingolipid deficiency activates ERK in a pathway different from the PKC pathway. The mechanism by which sphingolipid deficiency causes ERK activation is not yet known; however, it is important to note that many raft-associated proteins mediate signal transduction (20, 45, 48) and that cholesterol depletion also stimulates ERK activity in neurons (49) and non-neuronal cells (50, 51). Interestingly, cholesterol deficiency is reported to increase sAPPα secretion level, although it is not clear whether the MAP/ERK pathway is involved in the cholesterol depletion-mediated increase in sAPPα secretion level (12). These lines of evidence suggest that altered levels of cholesterol or phospholipids in lipid rafts may affect the raft-mediated signal transduction pathway, ERK, leading to an increase in the sAPPα secretion level.

However, the possibility cannot be excluded that cholesterol and sphingolipid depletion enhances APP α-cleavage in a different manner, because previous reports suggested that disruption in the formation of lipid rafts and their clustering caused by the depletion of cholesterol in lipid rafts lead to the inhibition of APP partitioning into lipid rafts, a decrease in the β-cleavage activity, and an increase in α-cleavage activity of APP (7, 13). In contrast, our findings show that under the conditions in which cellular cholesterol level is unchanged, lipid raft dysfunctions caused by sphingolipid depletion may enhance the α-cleavage activity of APP without affecting the β-cleavage activity of APP or APP level in lipid rafts (Fig. 6*b*). These results imply that sphingolipid depletion may enhance APP α-cleavage activity without shifting the intracellular trafficking of APP from the Aβ-generating site (lipid rafts) to the Aβ-nongenerating site (outside lipid rafts). These results suggest that cholesterol and sphingolipids play entirely different roles in determining the properties of lipid rafts. In support of this notion, the effect of sphingolipid depletion opposite to that

of cholesterol depletion on the formation of the scrapie prion protein, which is assumed to occur in lipid rafts, was demonstrated (27, 52). However, the mechanism(s) underlying the different effects of cholesterol and sphingolipid depletion on APP processing remains unclarified, and further studies are required elucidate the regulation of α-secretase, ADAM 10 (a disintegrin and metalloprotease) (53), based on lipids present in rafts and outside lipid rafts.

Recently, it has been shown that ceramide enhances the biogenesis of Aβ by modulating APP β-cleavage (54). It was also shown that an increased level of cellular ceramide increases the level of α- and β-APP-CTFs, indicating that the sAPPα secretion level also increases. In our experiments, sAPPα secretion level increased in the cells in which the levels of sphingolipid including ceramide are reduced. One cannot explain this discrepancy at present; however, it may be possible that the profiles of the cellular levels of phospholipids in our experiments and others are different. For example, both ISP-1 (our study) and fumonisine B1 (54) reduce the cellular levels of ceramide, glycosphingolipids, and sphingomyelin; however, fumonisine B1 increases the level of dehydrosphingosine, which is a precursor of ceramide, whereas ISP-1 reduces its level. Because dehydrosphingosine has various biological effects on cells such as PKC activity (55), the different effect of fumonisine B1 from that of ISP-1 on the dehydrosphingosine level may in part explain the contradictory result of sAPPα secretion caused by fumonisine B1 to that induced by ISP-1 and SPT deficiency.

Our data show that an increase in the level of secreted Aβ42 is accompanied by a decreased activity of APP ϵ-cleavage in sphingolipid-deficient cells, supporting in part our previous finding that Aβ42-specific elevation accompanied by the significant reduction of sphingolipids in lipid rafts are noted in the mutant presenilin 2 transgenic mouse brains (33). Interestingly, the different effects of sphingolipid deficiency on Aβ42 generation and APP ϵ-cleavage agree with the findings reported in previous studies using cells with PS mutations (56, 57). In those studies, it was shown that an increase in the level of APP γ42-cleavage is accompanied by a decrease in the ϵ-cleavage level in various PS1 mutant cells. These data suggest that γ-secretase at residue 42 and ϵ-cleavage are likely to be reciprocally regulated in PS mutant cells and that cellular sphingolipids may be involved in these regulations. It has been also shown that the activation of PKC stimulates α-cleavage of APP at the expense of β-secretase cleavage (58–60). In contrast, other studies demonstrated that PKC activation enhances sAPPα release without decreasing Aβ production (43, 61, 62). Similarly, cholesterol depletion increases sAPPα secretion level and reduces Aβ production (7, 12, 13), whereas the data presented here indicate that the phospholipid deficiency-induced activation of ERK enhances sAPPα secretion, although it does not inhibit Aβ generation but rather increases Aβ42 secretion level. These different results provide evidence of the sAPPα production and of Aβ being derived from distinct metabolic pathways that can be differently regulated by cholesterol or phospholipids.

Finally, our present study raises the caution that not only cholesterol but also sphingolipids should be focused on when one discusses the relationship between lipid rafts and AD development. Further studies are required to clarify whether PS mutations alter the sphingolipid metabolism and whether alterations in sphingolipid metabolism are associated with sporadic AD development. However, our observations in the present study provide a new insight into one of the central issues concerning AD pathogenesis, that is, the relationship between altered lipid metabolism and the development of AD.

Acknowledgments—We thank E. H. Koo for providing the CHO-K1 cell line expressing APP751 and Takeda Chemical Industries, Ltd. for providing antibodies, BNT77, BA27, and BC05.

REFERENCES

1. Buxbaum, J. D., Oishi, M., Chen, H. I., Pinkas-Kramarski, R., Jaffe, E. A., Gandy, S. E., and Greengard, P. (1992) *Proc. Natl. Acad. Sci. U. S. A.* **89,** 10075–10078
2. Nitsch, R. M., Slack, B. E., Wurtman, R. J., and Growdon, J. H. (1992) *Science* **258,** 304–307
3. Caporaso, G. L., Gandy, S. E., Buxbaum, J. D., Ramabhadran, T. V., and Greengard, P. (1992) *Proc. Natl. Acad. Sci. U. S. A.* **89,** 3055–3059
4. Mills, J., Laurent Charest, D., Lam, F., Beyreuther, K., Ida, N., Pelech, S. L., and Reiner, P. B. (1997) *J. Neurosci.* **17,** 9415–9422
5. Schubert, D., Jin, L. W., Saitoh, T., and Cole, G. (1989) *Neuron* **3,** 689–694
6. Weidemann, A., Eggert, S., Reinhard, F. B., Vogel, M., Paliga, K., Baier, G., Masters, C. L., Beyreuther, K., and Evin, G. (2002) *Biochemistry* **41,** 2825–2835
7. Simons, M., Keller, P., De Strooper, B., Beyreuther, K., Dotti, C. G., and Simons, K. (1998) *Proc. Natl. Acad. Sci. U. S. A.* **95,** 6460–6464
8. Bodovitz, S., and Klein, W. L. (1996) *J. Biol. Chem.* **271,** 4436–4440
9. Racchi, M., Baetta, R., Salvietti, N., Ianna, P., Franceschini, G., Paoletti, R., Fumagalli, R., Govoni, S., Trabucchi, M., and Soma, M. (1997) *Biochem. J.* **322,** 893–898
10. Simons, M., Keller, P., Dichgans, J., and Schulz, J. B. (2001) *Neurology* **57,** 1089–1093
11. Hartmann, T. (2001) *Trends Neuorsci.* **24,** S45–S48
12. Kojro, E., Gimpl, G., Lammich, S., Marz, W., and Fahrenholz, F. (2001) *Proc. Natl. Acad. Sci. U. S. A.* **98,** 5815–5820
13. Ehehalt, R., Keller, P., Haass, C., Thiele, C., and Simons, K. (2003) *J. Cell Biol.* **160,** 113–123
14. Morishima-Kawashima, M., and Ihara, Y. (1998) *Biochemistry* **37,** 15247–15253
15. Lee, S. J., Liyanage, U., Bickel, P. E., Xia, W., Lansbury, P. T., Jr., and Kosik, K. S. (1998) *Nat. Med.* **4,** 730–734
16. Li, Y. M., Xu, M., Lai, M. T., Huang, Q., Castro, J. L., DiMuzio-Mower, J., Harrison, T., Lellis, C., Nadin, A., Neduvelil, J. G., Register, R. B., Sardana, M. K., Shearman, M. S., Smith, A. L., Shi, X. P., Yin, K. C., Shafer, J. A., and Gardell, S. J. (2000) *Nature* **405,** 689–694
17. Riddell, D. R., Christie, G., Hussain, I., and Dingwall, C. (2001) *Curr. Biol.* **11,** 1288–1293
18. Wahrle, S., Das, P., Nyborg, A. C., McLendon, C., Shoji, M., Kawarabayashi, T., Younkin, L. H., Younkin, S. G., and Golde, T. E. (2002) *Neurobiol. Dis.* **9,** 11–23
19. Simons, K., and Ikonen, E. (1997) *Nature* **387,** 569–572
20. Brown, D. A., and London, E. (2000) *J. Biol. Chem.* **275,** 17221–17224
21. Anderson, R. G. (1998) *Annu. Rev. Biochem.* **67,** 199–225
22. Hanada, K., Izawa, K., Nishijima, M., and Akamatsu, Y. (1993) *J. Biol. Chem.* **268,** 13820–13823
23. Hanada, K., Nishijima, M., Akamatsu, Y., and Pagano, R. E. (1995) *J. Biol. Chem.* **270,** 6254–6260
24. Stevens, V. L., and Tang, J. (1997) *J. Biol. Chem.* **272,** 18020–18025
25. Vey, M., Pilkuhn, S., Wille, H., Nixon, R., DeArmond, S. J., Smart, E. J., Anderson, R. G., Taraboulos, A., and Prusiner, S. B. (1996) *Proc. Natl. Acad. Sci. U. S. A.* **93,** 14945–14949
26. Kaneko, K., Vey, M., Scott, M., Pilkuhn, S., Cohen, F. E., and Prusiner, S. B. (1997) *Proc. Natl. Acad. Sci. U. S. A.* **94,** 2333–2338
27. Naslavsky, N., Shmeeda, H., Friedlander, G., Yanai, A., Futerman, A. H., Barenholz, Y., and Taraboulos, A. (1999) *J. Biol. Chem.* **274,** 20763–20771
28. Hanada, K., Nishijima, M., Fujita, T., and Kobayashi, S. (2000) *Biochem. Pharmacol.* **59,** 1211–1216
29. Hanada, K., Hara, T., Fukasawa, M., Yamaji, A., Umeda, M., and Nishijima, M. (1998) *J. Biol. Chem.* **273,** 33787–33794
30. Asami-Odaka, A., Ishibashi, Y., Kikuchi, T., Kitada, C., and Suzuki, N. (1995) *Biochemistry* **34,** 10272–10278
31. Tomita, S., Ozaki, T., Taru, H., Oguchi, S., Takeda, S., Yagi, Y., Sakiyama, S., Kirino, Y., and Suzuki, T. (1999) *J. Biol. Chem.* **274,** 2243–2254
32. Oishi, M., Nairn, A. C., Czernik, A. J., Lim, G. S., Isohara, T., Gandy, S. E., Greengard, P., and Suzuki, T. (1997) *Mol. Med.* **3,** 111–123
33. Sawamura, N., Morishima-Kawashima, M., Waki, H., Kobayashi, K., Kuramochi, T., Frosch, M. P., Ding, K., Ito, M., Kim, T. W., Tanzi, R. E., Oyama, F., Tabira, T., Ando, S., and Ihara, Y. (2000) *J. Biol. Chem.* **275,** 27901–27908
34. Sawamura, N., Gong, J. S., Garver, W. S., Heidenreich, R. A., Ninomiya, H., Ohno, K., Yanagisawa, K., and Michikawa, M. (2001) *J. Biol. Chem.* **276,** 10314–10319
35. Hanada, K., Hara, T., Nishijima, M., Kuge, O., Dickson, R. C., and Nagiec, M. M. (1997) *J. Biol. Chem.* **272,** 32108–32114
36. Gu, Y., Misonou, H., Sato, T., Dohmae, N., Takio, K., and Ihara, Y. (2001) *J. Biol. Chem.* **276,** 35235–35238
37. Piiper, A., Elez, R., You, S. J., Kronenberger, B., Loitsch, S., Roche, S., and Zeuzem, S. (2003) *J. Biol. Chem.* **278,** 7065–7072
38. Lisanti, M. P., Scherer, P. E., Vidugiriene, J., Tang, Z., Hermanowski-Vosatka, A., Tu, Y. H., Cook, R. F., and Sargiacomo, M. (1994) *J. Cell Biol.* **126,** 111–126
39. Michikawa, M., Fan, Q. W., Isobe, I., and Yanagisawa, K. (2000) *J. Neurochem.* **74,** 1008–1016
40. Koo, E. H., and Squazzo, S. L. (1994) *J. Biol. Chem.* **269,** 17386–17389
41. Sastre, M., Steiner, H., Fuchs, K., Capell, A., Multhaup, G., Condron, M. M., Teplow, D. B., and Haass, C. (2001) *EMBO Rep.* **2,** 835–841
42. Nitsch, R. M., Deng, M., Growdon, J. H., and Wurtman, R. J. (1996) *J. Biol. Chem.* **271,** 4188–4194
43. Desdouits-Magnen, J., Desdouits, F., Takeda, S., Syu, L. J., Saltiel, A. R.,

Buxbaum, J. D., Czernik, A. J., Nairn, A. C., and Greengard, P. (1998) *J. Neurochem.* **70,** 524–530
44. Fukasawa, M., Nishijima, M., Itabe, H., Takano, T., and Hanada, K. (2000) *J. Biol. Chem.* **275,** 34028–34034
45. Simons, K., and Toomre, D. (2000) *Nat. Rev. Mol. Cell. Biol.* **1,** 31–39
46. Mudher, A., Chapman, S., Richardson, J., Asuni, A., Gibb, G., Pollard, C., Killick, R., Iqbal, T., Raymond, L., Varndell, I., Sheppard, P., Makoff, A., Gower, E., Soden, P. E., Lewis, P., Murphy, M., Golde, T. E., Rupniak, H. T., Anderton, B. H., and Lovestone, S. (2001) *J. Neurosci.* **21,** 4987–4995
47. Avramovich, Y., Amit, T., and Youdim, M. B. (2002) *J. Biol. Chem.* **277,** 31466–31473
48. Paratcha, G., and Ibanez, C. F. (2002) *Curr. Opin. Neurobiol.* **12,** 542–549
49. Sawamura, N., Gong, J.-S., Chang, T.-Y., Yanagisawa, K., and Michikawa, M. (2003) *J. Neurochem.* **84,** 1086–1096
50. Furuchi, T., and Anderson, R. G. (1998) *J. Biol. Chem.* **273,** 21099–21104
51. Wang, P. Y., Liu, P., Weng, J., Sontag, E., and Anderson, R. G. (2003) *EMBO J.* **22,** 2658–2667
52. Taraboulos, A., Scott, M., Semenov, A., Avrahami, D., Laszlo, L., Prusiner, S. B., and Avraham, D. (1995) *J. Cell Biol.* **129,** 121–132
53. De Strooper, B., and Annaert, W. (2000) *J. Cell Sci.* **113,** 1857–1870
54. Puglielli, L., Ellis, B. C., Saunders, A. J., and Kovacs, D. M. (2003) *J. Biol. Chem.* **278,** 19777–19783
55. Hannun, Y. A., Loomis, C. R., Merrill, A. H., Jr., and Bell, R. M. (1986) *J. Biol. Chem.* **261,** 12604–12609
56. Chen, F., Gu, Y., Hasegawa, H., Ruan, X., Arawaka, S., Fraser, P., Westaway, D., Mount, H., and St George-Hyslop, P. (2002) *J. Biol. Chem.* **277,** 36521–36526
57. Sato, T., Dohmae, N., Qi, Y., Kakuda, N., Misonou, H., Mitsumori, R., Maruyama, H., Koo, E. H., Haass, C., Takio, K., Morishima-Kawashima, M., Ishiura, S., and Ihara, Y. (2003) *J. Biol. Chem.* **278,** 24294–24301
58. Gabuzda, D., Busciglio, J., and Yankner, B. A. (1993) *J. Neurochem.* **61,** 2326–2329
59. Buxbaum, J. D., Koo, E. H., and Greengard, P. (1993) *Proc. Natl. Acad. Sci. U. S. A.* **90,** 9195–9198
60. Hung, A. Y., Haass, C., Nitsch, R. M., Qiu, W. Q., Citron, M., Wurtman, R. J., Growdon, J. H., and Selkoe, D. J. (1993) *J. Biol. Chem.* **268,** 22959–22962
61. Fuller, S. J., Storey, E., Li, Q. X., Smith, A. I., Beyreuther, K., and Masters, C. L. (1995) *Biochemistry* **34,** 8091–8098
62. LeBlanc, A. C., Koutroumanis, M., and Goodyer, C. G. (1998) *J. Neurosci.* **18,** 2907–2913

Neurodegenerative Disorders and Cholesterol

Makoto Michikawa*

Department of Alzheimer's Disease Research, National Institute for Longevity Sciences, 36-3 Gengo, Morioka, Obu, Aichi 474-8522, Japan

Abstract: It has been suggested that a high serum cholesterol level is a risk factor for Alzheimer's disease (AD), that treatment with cholesterol-lowering drugs (statins) reduces the frequency of AD development, and that the polymorpholism of genes encoding proteins regulating cholesterol metabolism is associated with the frequency of AD development. However, the mechanism by which high serum cholesterol level leads to AD, still remains unclarified. Several recent studies have shown the results challenging the above notions. Here another notion is proposed, that is, a low high-density lipoprotein (HDL) level in serum and cerebro-spinal fluid (CSF) is a risk factor for the development of AD; moreover, the possibility that AD and Niemann-Pick type C disease share a common cascade, by which altered cholesterol metabolism leads to neurodegeneration (tauopathy) is discussed. In this review, the association between cholesterol and AD pathogenesis is discussed from different viewpoints and several basic issues are delineated and addressed to fully understand the mechanisms underlying this relationship.

Keywords: Alzheimer's disease, cholesterol, Niemann-Pick type C disease, tauopathy, neurodegeneration, HDL, apolipoprotein E, lipid rafts.

INTRODUCTION

Studies on the metabolism of lipids including cholesterol have been performed for decades; however, the number of studies on cholesterol metabolism in the central nervous system (CNS) has been limited, although the brain is the most cholesterol-rich organ in the human body. Cholesterol metabolism in the CNS is segregated from the systemic circulation by the blood brain barrier; the lipoprotein found in the CNS is only high-density lipoprotein (HDL) and its concentration found in the CNS is lower than that in the systemic circulation. Therefore, one should obtain a better understanding of cholesterol metabolism and its significant roles in the CNS before discussing the relationship between cholesterol and neurodegerenative diseases. Another important point is that the morphological characteristics of neurons are markedly different from those of other cell types, which may allow cholesterol to play a specific and unique role in neurons. For example, the ratios of the total surface areas of the soma:dendrite:axon were estimated to be 1:65:845 in spinal motor neurons and 1:28:6 in hippocampal dentate granule cells, suggesting the importance of cholesterol circulation mediated by HDL, for example, in the nerve terminals. The very high turnover in synaptic remodeling (>20% of postsynaptic density clusters turns over within 24 h) has been demonstrated in hippocampal neurons [34] and that HDL cholesterol plays a key role in synaptogenesis and the maintenance of synapse plasticity in the hippocampus [27]. These findings suggest the critical role of HDL in cholesterol transport in the CNS. In this review article, taking these neuron- and CNS-specific characteristics into account, the association between cholesterol and neurodegenerative diseases including Alzheimer's disease (AD) and Niemann-Pick disease type C (NPC) is discussed.

*Address correspondence to this author at the Department of Alzheimer's Disease Research, National Institute for Longevity Sciences 36-3, Gengo, Morioka, Obu, Aichi 474-8522, Japan; Tel: 81 (0)562 46 2311; Fax: 81 (0)562 46 3157; E-mail: michi@nils.go.jp

I. CHOLESTEROL AND ALZHEIMER'S DISEASE

There have been reports linking the prevalence of Alzheimer's disease (AD) with the polymorphisms of genes related to cholesterol metabolism, including *apolipoprotein E* (*apoE*) [38, 45], *ABCA1* [52], and *CYP46*, the gene encoding cholesterol 34-hydroxylase, [22, 36]. In addition, it has been reported that the order of serum LDL and total cholesterol levels in the serum with respect to the *apoE* genotype is *apoE2<apoE3<apoE4* [4, 5, 7, 15, 24]. Epidemio-logical studies have suggested that an elevated serum total cholesterol level would be a risk factor for the development of AD and mild cognitive impairment (MCI) [20,33]. These findings suggest that those who have the *apoE* allele 4 develop AD earlier than those with other *apoE* genotypes due to the high levels of serum total cholesterol in these *apoE4* carriers. Moreover, since brain cholesterol is assumed to be converted to 24S-hydroxylcholesterol, an oxysterol that can diffuse across the blood-brain barrier into the systemic circulation, it is important to note that the 24-hydroxyl-cholesterol level in cerebrospinal fluid is elevated in the early stages of dementia [35] and statin treatment reduces the level in AD patients [48]. Several studies support these findings by showing that a reduced cellular cholesterol level reduces amyloid β-protein (Aβ) generation and stimulates the secretion of soluble amyloid precursor protein (APP) cleaved at the α site of APP (sAPPα) *in vitro* [21, 43] and *in vivo* [13]. However, these biochemical studies do not clarify the mechanism underlying the finding of epidemiological studies that "a high serum cholesterol level may be associated with a high frequency of AD development", because what they have shown is "a reduced

1567-2050/04 $45.00+.00

serum or cellular cholesterol level decreases Aβ secretion". Since cellular free cholesterol levels are strictly regulated, it is difficult to increase free cholesterol level in cells. In this meaning, the finding that cholesteryl-ester levels directly correlate with Aβ level [39] seems to be relevant to processes occuring in AD brains. How cholesterol level in the serum correlates to that in the CNS remains undetermined, and the molecular mechanism by which a high serum cholesterol level induces AD pathogenesis in the CNS has not been fully elucidated. Recently, a large, population-based cohort study has shown that there is no significant association between AD development and long-term average serum cholesterol level [47]. Recently a study has shown that γ-secretase mediated cleavage of APP required for generating Aβ occurs in rafts, but its activity is cholesterol-independent [49]. Previous papers reported that cholesterol level in the serum has no correlation with that in the CSF [9], cholesterol-rich diet has no effects on cholesterol level in CSF [19], and statin treatment does not decrease Aβ level in CSF although it decreases cholesterol level in CSF [14]. These findings reasonably raise the question of how one can explain the mechanism by which a high serum cholesterol level, which does not affect on cholesterol level in the CNS, modulates the pathogenesis of AD in the CNS. The observation that the level of Aβ in CSF remains unchanged, while that of cholesterol is decreased in patients treated with statins [14], suggests that the effect of statin, if any, of reducing the frequency of AD development cannot be explained by the reduced level of cholesterol in CSF and the subsequent inhibition of Aβ synthesis.

These lines of evidence indicate that many issues should be clarified before one can determine the association between cholesterol and AD. It should be noted that almost all of the studies mentioned above focused on cholesterol level in the systemic circulation and not that in the CNS. There should be a distinct difference in cholesterol metabolism between the systemic circulation and CNS, due to the separation of these two systems by the blood-brain barrier. One of the differences is that although several types of lipoprotein exist in serum, only HDL can be found in the CNS [9, 37]. It was shown that the levels of HDL cholesterol in the CNS are apoE-isoform-specific in the order of apoE2>apoE3>apoE4 [5, 15], which is the reverse order for the levels of total and LDL cholesterol [4, 5, 7, 24]. This apoE specificity can be explained by the isoform-dependent generation of HDL as a lipid acceptor [16,30]. Although there are few studies on cholesterol level in CSF, these lines of evidence suggest that HDL cholesterol levels in CSF of patients with AD are lower than those of the control. Previous studies showed that the level of HDL cholesterol in CSF of patients is lower than that of the control [18, 28], suggesting that a low HDL cholesterol level in the CSF may be a risk factor for AD development [29]. It was also reported that statin enhances HDL generation [1, 3, 6], supporting this notion. However, recent studies have shown that the level of serum 24-hydroxylcholesterol is elevated in patients with AD [35, 42], and that intronic CYP46 polymorphism is associated with AD [36], and that the single-nucleotide polymorphism of the *ABCA1* gene is associated with a low level of CSF cholesterol and a delayed onset of AD [52], implying that a high cholesterol level in the CNS may be involved in AD development. Taken together, further studies are still required to clarify in detail how cholesterol metabolism in the serum is associated with cholesterol metabolism in the CNS, and how altered cholesterol metabolism in the CNS enhances Aβ generation leading to AD development.

II. ROLE OF CHOLESTEROL IN NEURODEGENERATION

The formation of neurofibrillary tangles (NFTs) consisting of the hyperphosphorylation of tau is considered to be one of the major pathological hallmarks in the AD brain. However, the mechanisms underlying the accelerated phosphorylation of tau and the subsequent formation of NFTs in the AD brain remain unclarified. In this context, it is interesting to note that an altered cholesterol metabolism and NFT formation coexist in the brains with Niemann-Pick type C disease [2, 26, 46] without the deposition of senile plaques. These lines of evidence suggest that an abnormal cholesterol metabolism contributes to the development of tauopathy in the absence of Aβ aggregation in NPC. We found that tau in the brains of an NPC mouse model is hyperphosphorylated in a site-specific manner [41], which is accompanied by an enhanced activity of mitogen-activated kinase (MAPK), and that MAPK activation in NPC is induced by a decreased level of cholesterol in the plasma membrane and in lipid rafts [40]. This is also the case for primary cultures neurons [11] and *in vivo* brain slices [23]. Supporting these findings, a recent study has demonstrated that the acute depletion of membrane cholesterol results in the marked increase in the level of pERK1/2 in caveola/raft lipid domains and the cytosol of human fibroblasts, which is regulated by phosphatase that dephosphorylates both the phosphotyrosine and phosphothreonine residues of ERK1/2. [50]. These results indicate that the tau phosphorylation state is modulated by cholesterol in specific cellular compartments such as lipid rafts, leading to an altered intracellular signaling. Interestingly, a deficiency in cellular cholesterol or a deficiency in cholesterol supply in neurons was shown to inhibit dendritic outgrowth [12] and synaptogenesis [23, 27], and induce neurodegeneration [32], as well as tauopathy [11, 23, 40, 41]. These findings suggest that AD and NPC share a common pathological pathway, by which altered cholesterol metabolism leads to tauopathy (Fig. **1**). In accordance with this notion, a recent review discussed a similar idea that Aβ kills neurons by inhibiting cholesterol synthesis and that statins acting at the neuronal level could further exacerbate neurodegeneration in AD by inhibiting the necessary cholesterol synthesis [44].

It is noteworthy that oligomeric Aβ affects cellular cholesterol metabolism [25, 31] by generating Aβ-lipid particles with a density identical to that of HDL, which cannot be internalized into cells [31]. Importantly, oligomeric but not monomeric Aβ reduces cholesterol level in neurons [17]. These findings imply the central role of cholesterol in the amyloid cascade (see review [10]) (Fig. **1**); that is, an increased level of Aβ oligomers affects cellular cholesterol metabolism, resulting in the reduction in cholesterol level in neurons, which in turn induces the hyperphosphorylation of tau, the impairment of synaptic plasticity, and finally neurodegeneration.